AD-A151 553 SPECTROSCOPIC STUDIES OF LASING TRANSITIONS IN THE DIATOMIC MERCURY HALIDES(U) VANDERBILT UNIV NASHVILLE TN DEPT OF CHEMISTRY J TELLINGHUISEN FEB 85 1/1

UNCLASSIFIED N00014-81-K-0477 F/G 7/4 NL

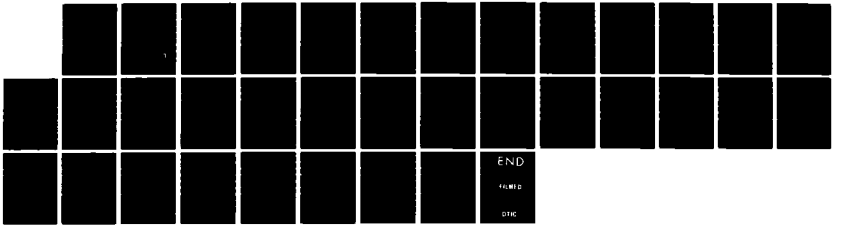

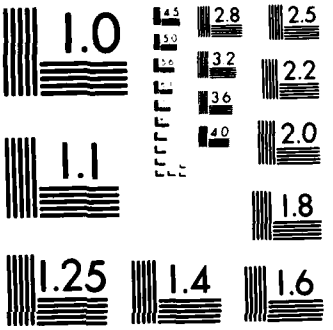

Report N00014-81-K-0477-3

AD-A151 553

SPECTROSCOPIC STUDIES OF LASING TRANSITIONS IN THE DIATOMIC MERCURY HALIDES

Joel Tellinghuisen
Department of Chemistry
Vanderbilt University
Nashville, Tennessee 37235

February, 1985

Final Report for Period May 1, 1981 to September 30, 1984

Approved for public release; distribution unlimited

Prepared for:

Office of Naval Research
Physics Division Office (Code 412)
800 North Quincy Street
Arlington, Virginia 22217

SECURITY CLASSIFICATION OF THIS PAGE (When Data Entered)

REPORT DOCUMENTATION PAGE	READ INSTRUCTIONS BEFORE COMPLETING FORM
1. REPORT NUMBER: N00014-81-K-0477-3	2. GOVT ACCESSION NO.: AD-A151553
3. RECIPIENT'S CATALOG NUMBER	
4. TITLE (and Subtitle): SPECTROSCOPIC STUDIES OF LASING TRANSITIONS IN THE DIATOMIC MERCURY HALIDES	5. TYPE OF REPORT & PERIOD COVERED: Final -- May 1, 1931 - September 30, 1984.
	6. PERFORMING ORG. REPORT NUMBER
7. AUTHOR(s): Joel Tellinghuisen	8. CONTRACT OR GRANT NUMBER(s): N00014-81-K-0477
9. PERFORMING ORGANIZATION NAME AND ADDRESS: Department of Chemistry, Vanderbilt University, Nashville, Tennessee 37235	10. PROGRAM ELEMENT, PROJECT, TASK AREA & WORK UNIT NUMBERS: PEN: 61153N, P-TAN: RR011-07-01, WUN: NR 395-612
11. CONTROLLING OFFICE NAME AND ADDRESS: Office of Naval Research, Physics Division Office (Code 412), 800 North Quincy Street, Arlington, Virginia 22217	12. REPORT DATE: February, 1985
	13. NUMBER OF PAGES: 32
14. MONITORING AGENCY NAME & ADDRESS(if different from Controlling Office)	15. SECURITY CLASS. (of this report): Unclassified
	15a. DECLASSIFICATION/DOWNGRADING SCHEDULE

16. DISTRIBUTION STATEMENT (of this Report)

Approved for public release; distribution unlimited

17. DISTRIBUTION STATEMENT (of the abstract entered in Block 20, if different from Report)

18. SUPPLEMENTARY NOTES

19. KEY WORDS (Continue on reverse side if necessary and identify by block number)

mercury halides, xenon fluoride, HgCl, HgBr, HgI, XeF, electronic transition lasers, electronic spectroscopy, diatomic spectroscopy, vibrational analysis, rotational analysis, emission spectroscopy, potential curves, Franck-Condon factors, partition functions.

20. ABSTRACT (Continue on reverse side if necessary and identify by block number)

The B - X, C - X, and D - X emission transitions of HgCl, HgBr, and HgI and the B - X transition of XeF have been photographed and analyzed for isotopically pure HgX and XeF molecules. New methods have been devised for fitting data and approximating potential curves for heavy diatomics like these molecules. Results of the analyses for these molecules offer significant improvements in their spectroscopic parameters and related properties, such as potential curves, Franck-Condon factors, dissociation energies and partition functions.

DD FORM 1 JAN 73 1473 EDITION OF 1 NOV 65 IS OBSOLETE

S N 0102-LF-014-6601

SECURITY CLASSIFICATION OF THIS PAGE (When Data Entered)

Research Summary

The research performed under this project has emphasized an improved characterization of the spectroscopic properties of the diatomic mercury halide molecules. The work has employed mainly conventional methods of high-resolution emission spectroscopy, coupled with the use of "cool" Tesla discharge sources containing single isotopomers (e.g. $^{200}Hg^{79}Br$). The use of isotopically pure ^{200}Hg in these sources has led to considerable simplification of the emission spectra, from elimination of the isotopic blending that results from vibrational isotope shifts in "natural" HgX sources. The primary targets of these studies have been the $B \rightarrow X$ emission systems, which occur in the visible region of the spectrum and serve as the lasants in the mercury halide "blue-green" lasers. However, our more recent work has included reanalysis of UV emission systems in these molecules, in order to improve the description of the HgX ground states at low v, where they are not accessed in emission from the B states under the conditions of our discharges (and of HgX lasers).

These studies have led to extensive revisions in the vibrational assignments of bands which occur in the most intense region of the HgX $B \rightarrow X$ spectra, which are the regions relevant to the HgX lasers. One outcome of these revisions is a lowering (by about 10%) of the estimated dissociation energies of the ground (X) states of these molecules. Accordingly the potential curves for these states are altered from their previous assessment, and with them the calculated Franck-Condon factors for $B \rightarrow X$ emission from low v' levels. The new FCFs are more in keeping with the observed features in the laser spectra, although there is still no simple assignment of the latter. Rather they appear to be associated with chance coincidences of many rotational lines in the densely overlapped spectra of the multiple isotopomers occurring in the "natural" HgX molecules employed in the laser experiments. Several papers have been published on this work (items 1,2,6-8 under "Publications" below) and more are anticipated (see Appendices 4 and 5).

In connection with our study of the HgX emission spectra, we have developed new methods for analyzing spectra of heavy diatomic molecules. In such molecules electronic spectra tend to be very congested, even for relatively low discharge temperatures. This congestion is a direct consequence of the small vibrational and rotational frequencies which always occur in diatomics with large reduced masses; and it makes a rotational analysis difficult or practically impossible. On the other hand the vibrational

structure in such spectra may be rich, leading to quite good determination of the vibrational constants. We have found that it is possible to obtain fairly reliable potential curves for electronic states involved in such congested transitions, by using a Morse approximation to represent the unknown left or repulsive branch of the potential, and the RKR f integrals (which require only the vibrational constants) to calculate the *width* of the potential -- and hence the right or attractive branch -- as a function of v and the vibrational energy G_v. A paper describing this method has been published (item 3 under "Publications" below).

Another method we have developed is the use of "mixed" representations for rotational and vibrational constants of diatomics. It is well known that polynomials in $(v + 1/2)$ are very efficient for representing B_v and G_v data for diatomics at low-to-moderate v. However, near dissociation such polynomials are not well behaved and they become very inefficient. In this regime so-called near-dissociation expansions (NDEs), which represent the energy and rotational constant in a theoretically sound way with the dissociation limit as reference, become very efficient. However, NDEs are no better at low v than are polynomials in $(v + 1/2)$ at high v. Hence we have experimented with mixed representations -- polynomials for low v, NDEs for high -- and have found them to perform quite well in our test calculations on HgBr(X). A paper describing this method has been published (Publication 8) and represents an extension of earlier work on NDEs (see Publication 5).

As a spin-off of our work on efficient representations of spectroscopic data for diatomics, we have also developed new methods for calculating diatomic partition functions. These methods are particularly useful for dealing with electronic states which are only weakly bound, such that significant contributions to the partition function (and hence to the thermodynamic properties) come from levels near dissociation. One of the new methods can be considered exact; it employs efficient Gaussian quadrature schemes to evaluate the semiclassical eigenvalues for a given potential curve, and then evaluates the partition function as a direct sum of the Boltzmann factors for these levels. The second method employs classical phase integrals to evaluate rotation-vibration partition functions about two orders of magnitude faster than the semiclassical procedure, with a reliability of about 1% when kT is greater than about twice the vibrational frequency. (This condition can occur at relatively low T for heavy diatomics.) These methods have been described in

two published papers (Publications 10 and 12, included as Appendices 1 and 3 of this report).

In an extension of the original program of research on the HgX molecules, we have also worked on the analysis of the *B→X* spectrum of $^{136}Xe^{19}F$. This work was supported by DARPA and led to a publication of an updated and refined analysis of the XeF laser spectrum (Publication 11 and Appendix 2).

Continuing Work

We have accomplished the main goals of this project -- namely the reanalysis of the emission spectra of HgCl, HgBr, and HgI. Brief reports on this work have been published, and the full papers describing the work on HgI and HgBr are now in preparation for publication in the *Journal of Molecular Spectroscopy*. Most of the tables to be included in these papers have been prepared and are included with this report as Appendices 4 and 5. In the case of HgCl the rotational analysis of *B→X* remains to be done. This work should be completed by September, 1985; it too will be published in the *Journal of Molecular Spectroscopy*.

In the extension work on XeF we have also succeeded in the main goal of completing the rotational analysis of the *B→X* spectrum of $^{136}Xe^{19}F$. Here too questions remain, particularly as regards the possibility of *B-C* perturbations, which should occur but which have not yet been identified in our spectra. Again a brief report of this work has appeared, and the full publication is planned for the *Journal of Molecular Spectroscopy*.

Initially we intended to conduct transient absorption experiments on the HgX molecules in order to characterize the *B→X* absorption from low v'' levels to high v' levels -- the region ***not*** sampled in *B→X* emission. However we opted for a reanalysis of the UV emission spectra (primarily *C→X* and *D→X*) instead, as these transitions nicely determine the low-v regions of the ground states. This work has led to greatly improved descriptions of the ground states, including their thermodynamic properties in the case of HgBr (Publication 12). We expect to publish papers on the partition functions and thermodynamic properties of HgI, HgCl, and XeF, also, when the fundamental spectroscopy papers on these molecules have been completed.

There is one element of our project in which we have failed to accomplish our goals. That is the intended study of pressure broadening of rotational lines in the HgX and XeF *B→X* spectra. To date we have been unable to conduct

very high resolution measurements with our Fabry-Perot interferometer, which we had hoped to couple with our spectrometer to study line widths. Although we have not abandoned this goal, it is clear that success in this area will require time and effort beyond the realm of this project, so this work will not be completed in the foreseeable future.

In another area -- the study of pressure and temperature dependence of the HgX emission spectra -- we have done some work (see Publications 7 and 9) but will probably not complete the calculations needed to estimate vibrational relaxation rates and the R-dependence of the B-X transition moment function. As work progressed on the analysis of the spectra, it became clear that this aspect of the study could provide only rough estimates at best; consequently it was relegated to low priority.

Personnel

Three graduate students -- K. S. Viswanathan, J. Gail Ashmore, and O. Carlysle Salter -- have been employed essentially full time on this project. Dr. Viswanathan has completed the requirements for his Ph. D. degree (thesis: "Part 1: Spectroscopic Studies of Charge Transfer Transitions in Iodine, Bromine, and Mercury Iodide; Part 2: Nitrogen Laser Pumped Dye Laser," June, 1983), and has taken a postdoctoral appointment in the Department of Chemistry at the University of Indiana. Ashmore and Salter are now in their fifth years and expect to finish their theses before September, 1985. Three undergraduates have also been associated with the project: Patrick Berwanger, Sue A. Davies, and Stuart D. Henderson. Berwanger is currently employed with Exxon in Houston, Texas, and Davies and Henderson are in their senior years at Vanderbilt, with plans to continue their education in graduate school. Other personnel affiliated with the project were Patricia C. Tellinghuisen as Research Associate (part time) and myself.

Publications

1. "The $B \rightarrow X$ transition in $^{200}Hg^{79}Br$," by Joel Tellinghuisen and J. Gail Ashmore, *Appl Phys Lett* **40**, 867 (1982).
2. "$B \rightarrow X$ transitions in HgCl and HgI," by Joel Tellinghuisen, Patricia C. Tellinghuisen, Sue A. Davies, Patrick Berwanger, and K. S. Viswanathan, *Appl Phys Lett* **41**, 789 (1982).

3. "The Use of Morse-RKR Curves in Diatomic Calculations," by Joel Tellinghuisen and Stuart D. Henderson, *Chem Phys Lett* **91**, 447 (1982).
4. "Spectroscopic Studies of Lasing Transitions in the Diatomic Mercury Halides," by Joel Tellinghuisen (Annual summary report for period May 1, 1981 to April 30, 1982), Report N00014-81-K-0477-1, AD No. AD A116297.
5. "Direct Fitting of Spectroscopic Data to Near-Dissociation Expansions: $I_2(D'\rightarrow A')$, $Br_2(D'\rightarrow A')$, and XeCl ($B\rightarrow X$ and $D\rightarrow X$)," by Joel Tellinghuisen, *J Chem Phys* **78**, 2374 (1983).
6. "The $B(^2\Sigma^+) \rightarrow X(^2\Sigma^+)$ Transition (4050-4500 Å) in HgI," by K. S. Viswanathan and Joel Tellinghuisen, *J. Mol. Spectrosc* **98**, 185 (1983).
7. "Mercury Halide Spectroscopy," by Joel Tellinghuisen, in *Excimer Lasers-1983*, edited by C. K. Rhodes, H. Egger, and H. Pummer (AIP Conference Proceedings Number 100, AIP, New York, 1983), p. 99.
8. "Mixed Representations for Diatomic Spectroscopic Data: Application to HgBr," by Joel Tellinghuisen and J. Gail Ashmore, *Chem Phys Lett* **102**, 10 (1983).
9. "Spectroscopic Studies of Lasing Transitions in the Diatomic Mercury Halides," by Joel Tellinghuisen (Annual summary report for period May 1, 1982 to April 30, 1983), Report N00014-81-K-0477-2.
10. "Diatomic Partition Functions from Semiclassical Phase Integrals," by Joel Tellinghuisen, *Chem Phys Lett* **102**, 4 (1983). (Appendix 1)
11. "$B\rightarrow X$ transition in $^{136}Xe^{19}F$," by Patricia C. Tellinghuisen and Joel Tellinghuisen, *Appl Phys Lett* **43**, 898 (1983). (Appendix 2)
12. "Diatomic Partition Functions from Classical and Semiclassical Phase Integrals," by Joel Tellinghuisen, *High Temp Sci* **17**, 289 (1984). (Appendix 3)
13. "Spectroscopic Studies of Lasing Transitions in the Diatomic Mercury Halides," by Joel Tellinghuisen (Final Report, this document), Report N00014-81-K-0477-3.

Conference Papers

1. "The B→X Transition in $^{200}Hg^{79}Br$," by J. Gail Ashmore and Joel Tellinghuisen, 37th Symposium on Molecular Spectroscopy (Columbus, Ohio), June, 1982.
2. "The B→X Transition in HgI," by K. S. Viswanathan and Joel Tellinghuisen, 37th Symposium on Molecular Spectroscopy (Columbus, Ohio), June, 1982.

3. "The Use of Morse-RKR Curves in Diatomic Calculations," by Stuart D. Henderson and Joel Tellinghuisen, 37th Symposium on Molecular Spectroscopy (Columbus, Ohio), June, 1982.
4. "Reanalysis of the B→X Transitions in the Mercury Halides," by J. Tellinghuisen, P. C. Tellinghuisen, J. G. Ashmore, and K. S. Viswanathan, 35th Gaseous Electronics Conference (University of Texas at Dallas), October, 1982.
5. "Spectroscopic Studies of Diatomic Electronic Transition Lasers," by Joel Tellinghuisen, 34th Southeastern Regional American Chemical Society Meeting (Birmingham, Alabama), November, 1982.
6. "The Emission Spectrum of HgI," by K. S. Viswanathan, O. Carlysle Salter, and Joel Tellinghuisen, 92nd Meeting of the Tennessee Academy of Science (Martin, Tennessee), November, 1982.
7. "The Emission Spectrum of HgBr," by J. Gail Ashmore and Joel Tellinghuisen, 92nd Meeting of the Tennessee Academy of Science (Martin, Tennessee), November, 1982.
8. "Interfacing a Microdensitometer to a Microcomputer," by O. Carlysle Salter and Joel Tellinghuisen, 92nd Meeting of the Tennessee Academy of Science (Martin, Tennessee), November, 1982.
9. "The Use of Morse-RKR Curves in Diatomic Calculations," by Stuart D. Henderson and Joel Tellinghuisen, 92nd Meeting of the Tennessee Academy of Science (Martin, Tennessee), November, 1982.
10. "Mercury Halide Spectroscopy," by Joel Tellinghuisen, Topical Meeting on Excimer Lasers (Incline Village, Nevada), January, 1983.
11. " 'Best' Spectroscopic Constants for HgBr from Direct Fits of Multiple Band Systems to Polynomials and Near-Dissociation Expansions," by J. Gail Ashmore and Joel Tellinghuisen, 38th Symposium on Molecular Spectroscopy (Columbus, Ohio), June, 1983.
12. "Interfacing a Microdensitometer to a Microcomputer," by O. Carlysle Salter and Joel Tellinghuisen, 38th Symposium on Molecular Spectroscopy (Columbus, Ohio), June, 1983.
13. "Interfacing to a Radio Shack TRS-80 Microcomputer -- 1983 Update," by O. Carl Salter and Joel Tellinghuisen, 93rd Meeting of the Tennessee Academy of Science (Gallatin, TN), November, 1983.
14. "Diatomic Partition Functions from Classical and Semiclassical Phase Integrals," by Joel Tellinghuisen, 93rd Meeting of the Tennessee Academy of Science (Gallatin, TN), November, 1983.

Volume 102, number 1 CHEMICAL PHYSICS LETTERS 11 November 1983

DIATOMIC PARTITION FUNCTIONS FROM SEMICLASSICAL PHASE INTEGRALS

Joel TELLINGHUISEN
Department of Chemistry, Vanderbilt University, Nashville, Tennessee 37235, USA

Received 6 September 1983; in final form 15 September 1983

Diatomic rotation–vibration partition functions are evaluated through a technique which utilizes semiclassical phase integrals to estimate the eigenvalues. For the assessment of the contributions from the bound and metastable levels, the method is computationally efficient and virtually exact for any potential at any temperature.

1. Introduction

In statistical mechanics the traditional starting point for evaluating the internal partition function q_{vr} of a diatomic molecule is the combination of the rigid-rotor model for rotation and the harmonic oscillator for vibration [1]. The rigid-rotor/harmonic oscillator (RR/HO) partition function may then be corrected for effects of anharmonicity and vibration–rotation interaction through approximations [2] which are quite reliable for temperatures low enough that only the first few vibrational levels contribute significantly to q_{vr}. However, as kT becomes large compared to the vibrational energy, $hc\omega_e$, it becomes necessary to include levels beyond the range of validity of these approximations. In principle one can always calculate the "exact" q_{vr} from an explicit sum of Boltzmann factors over all energy levels, using spectroscopic constants to evaluate the latter. As long as only low-v levels are important, this approach is again satisfactory and straightforward to apply, because the partition function converges rapidly to its final value with inclusion of at most several hundred rotational levels for each of the several low-lying v levels. However, with increasing T it is necessary to include a rapidly increasing number of states in the sum, and certain problems may arise. First, of course, there is the obvious inconvenience of having to sum over many more levels. But more importantly, the range of included levels may exceed the range of the spectroscopic observations, so that the levels are no longer correctly represented by the spectroscopic constants. The latter problem is particularly severe near the dissociation limit, where the centrifugal distortion constants are important, and where it is also necessary to verify that the calculated levels actually exist in the discrete spectrum. Moreover, when discrete levels near dissociation are important, so are metastable levels (rotational resonances) and even the vibrational continuum, as Mies and Julienne have noted in an elegant treatment of the diatomic molecule in equilibrium with its parent atoms [3].

Diatomic spectroscopic constants are customarily expressed as polynomials in $v+\frac{1}{2}$ [4], which is a theoretically appropriate representation based on an expansion of the potential energy curve about its minimum [5]. Near the dissociation limit these polynomials are not well behaved, exacerbating the above-mentioned problems of evaluating q_{vr}. Recent work has shown that near-dissociation expansions – which contain as argument $v_D - v$, where v_D is the non-integer vibrational quantum number at dissociation – provide a theoretically correct approach to dissociation, with efficiency comparable to that of the traditional polynomials in $v+\frac{1}{2}$ [6–9]. Thus near-dissociation expansions offer considerable advantage in the calculation of partition functions when levels near dissociation are important. However one must still devise procedures for determining the range of existing levels for various values of the rotational quantum number J, and for checking the validity of the expressions used to evaluate them.

In an alternative approach one may start with a potential curve $U_0(R)$ for the molecule in question and

numerically evaluate the eigenvalues of the effective potential.

$$U_J(R) = U_0(R) + \beta J(J+1)/R^2 , \qquad (1)$$

where β is a constant containing the inverse of the reduced mass μ [4]. The rotationless potential $U_0(R)$ can be calculated from the spectroscopic constants by the RKR method, which as generally applied is a first-order semiclassical method, but which nonetheless yields potentials which usually are valid quantum mechanically to ≈ 1 cm^{-1} [10]. Furthermore the potential $U_0(R)$ so determined can be extrapolated to the dissociation limit D_e as reliably and more easily than can the various spectroscopic constants. And the information about the existence of levels near and above D_e is directly available from the potential: For a given J, energies above the rotational barrier (R_b, E_b) belong to the continuum, while energies below the barrier are discrete ($E < D_e$) or metastable ($E > D_e$).

Methods for calculating the eigenvalues and wavefunctions of the effective potential $U_J(R)$ have been available for decades [11–14] and can be accurate to better than 10^{-3} cm^{-1}. However, for a heavy molecule the numerical solution of the Schrödinger equation for all levels can be quite time-consuming, and also quite tedious to apply near D_e, where the potential flares out gently to approach the asymptote. Metastable levels require special considerations [3] but can usually be taken as discrete and evaluated by taking the outer limit of integration as R_b, the location of the barrier [15].

In the present paper I describe a method of calculating partition functions directly from potential curves, in which, however, the eigenvalues are obtained from the semiclassical phase integral,

$$h(v+\tfrac{1}{2}) = (8\mu)^{1/2} \int_{R_1}^{R_2} [E - U_J(R)]^{1/2}\, dR . \qquad (2)$$

This equation yields directly the (non-integral) vibrational quantum number v for any specified $E \leqslant E_b$, through the indicated integral of the radial momentum between the classical turning points, R_1 and R_2. The advantages of this method are several: (1) It is orders of magnitude faster than numerical solution of the Schrödinger equation, since the integrals in eq. (2) can be evaluated with part-per-million accuracy using as few as 16 points [16]; (2) it is straightforward to apply, since the range of integration is a precisely defined function of the energy; (3) when used with an RKR-produced $U_0(R)$, it is "exact", since it is simply the inverse of the first-order semiclassical RKR method [16]. As an illustration of these points I note that in one of the test cases described below, I evaluated more than 50000 eigenvalues and calculated partition functions at five temperatures – using double precision arithmetic and less than four minutes of CPU time on a DEC-1099 computer. Thus this method is clearly a practicable one. Moreover, although the present calculations deal with just the discrete and metastable contributions to q_{vr}, very similar computational methods can be used to evalute the continuum contributions [3].

2. Computational method

The main trick which makes the present semiclassical approach feasible is the use of the very efficient Gauss–Mehler quadrature to evaluate the phase integral in eq. (2) [16,17]:

$$[2/(R_2 - R_1)] \int_{R_1}^{R_2} [E - U_J(R)]^{1/2} dR \equiv \int_{-1}^{1} F(x)\, dx$$

$$\equiv \int_{-1}^{1} (1-x^2)^{1/2} F_w(x)\, dx \approx \sum_{i=1}^{n} H_i F_w(x_i) . \qquad (3)$$

Note that for a purely harmonic potential, $F_w(x)$ is a constant, and this quadrature becomes *exact for any n*. The weights $\{H_i\}$ and abscissa $\{x_i\}$ are simple trigonometric functions [18], which for efficiency are calculated once at the outset and stored for further use. To illustrate the power of this quadrature, I show in tables 1 and 2 the valuates of v_b, the vibrational quantum number at the energy of the barrier E_b, for selected J levels of the potentials used to approximate I_2 and Ar_2 in the test calculations discussed further below. It is clear that a 16-point quadrature is more than adequate in every case; in fact most of the time even *four* points are sufficient! In this regard it is worth noting that the evaluation of v_b is probably the most severe test of the quadrature, since the potential is much farther from harmonic over the R range needed for this calculation than it is for levels near the mini-

Table 1
Numerical evaluation of the vibrational quantum number at the energy of the rotational barrier, for the Morse potential approximating I_2

J	v_b					R_1	R_b	E_m	E_b
	$n = 4$	$n = 8$	$n = 16$	$n = 32$	$n = 64$				
100	109.38155	109.43360	109.43296	109.43291	109.43290	2.29872	6.96471	376.78	12546.76
400	69.50184	69.49030	69.48912	69.48903	69.48902	2.37733	4.89839	5869.08	13882.34
700	18.39314	18.38709	18.38651	18.38647	18.38646	2.64414	3.85477	17042.85	18670.06

Table 2
Numerical evaluation of the vibrational quantum number at the energy of the rotational barrier, for the 6–12 potential approximating Ar_2

J	v_b				R_1	R_b	E_m	E_b
	$n = 4$	$n = 8$	$n = 16$	$n = 32$				
1	7.14407	9.38068	9.48636	9.48640	3.34980	31.66656	0.12	100.01
10	7.61419	7.70673	7.70676	7.70676	3.36076	11.62462	6.55	100.47
30	4.05543	4.05558	4.05551	4.05551	3.45029	6.76853	54.55	111.33

mum. Also, near $E = E_b$ a given error in v may represent a relatively small error in the estimated eigenvalues, which anyway to not need to be evaluated with spectroscopic accuracy for the calculation of q_{vr}. For example, the two highest levels in the effective potential for $J = 1$ in table 2 are less than 1 cm^{-1} apart.

A second procedure I have used to save computational time takes advantage of the fact that eq. (2) gives v as a continuous function of E. Thus one can set up a grid of (v, E) values spanning the energy region $E_m \leqslant E \leqslant E_b$, where E_m is the energy at the minimum of $U_J(R)$, and then simply interpolate over this grid to determine the eigenvalues. In the test calculations discussed below, as few as seven points over a grid linear in E served to determine the energies of the important low-v levels within 0.01 cm^{-1}! (It is important to include the two end points, $(v_m = -0.5, E_m)$ and (v_b, E_b) in this grid.) With so few points the levels in the highest E segment were occasionally in error by $\approx$10 cm^{-1}; however at low T these levels are unimportant, and at high T the error is insignificant in its effect on q_{vr}. (At high T it is the *number* of bound levels and their degeneracies that are important, not their energies.)

With the above points in mind, the computational algorithm may be summarized as follows: (1) For a given J, construct the effective potential $U_J(R)$, and locate the minimum (R_m, E_m) and barrier (R_b, E_b); (2) subdivide the energy range into L equal intervals separated by $\Delta E = (E_b - E_m)/L$, and evaluate v at the $L + 1$ resulting values of E; (3) calculate the eigenvalues E_v for $v = 0, 1, 2, \ldots$ by interpolation, and evaluate their contributions, $(2J + 1) \exp(-E_v/kT_i)$, to q_{vr} at each of several specified temperatures, T_i; (4) repeat the procedure for $J = 0, 1, 2, \ldots$ until there is no bound level in the effective potential, which occurs at or slightly below the J value which gives no minimum in $U_J(R)$. This procedure exhausts the discrete and metastable contributions systematically, so that only the continuum contributions, which must be evaluated by other means [3], remain. Note that the discrete and metastable contributions can be accumulated separately in step (3) if that information is of interest.

3. Test calculations

I have tested this method on three potentials – a Morse approximation to the ground state of I_2 (ω_e

= 214 cm^{-1}, D_e = 12500 cm^{-1}, R_e = 2.667 Å), a Morse curve for a typical "light" molecule (μ = 8 amu, D_e = 50000 cm^{-1}, ω_e = 2000 cm^{-1}, R_e = 1.2 Å), and a 6–12 approximation for Ar_2 (μ = 20 amu, C_6 = -5.65×10^5 Å^6 cm^{-1}, $C_{12} = 7.98 \times 10^8$ Å^{12} cm^{-1}, for which R_e = 3.76 Å and D_e = 100.01 cm^{-1}). In each case I evaluated the phase integral in (2) over 4, 8, 16, ... points until consecutive estimates agreed within $\Delta v = 10^{-4}$. For the interpolation grid L = 6 proved adequate; and 4-point and 6-point Lagrangian interpolations gave identical values of q_{vr}. As noted earlier, the most computationally demanding of these tests was the I_2 calculation, in which some 5×10^4 eigenvalues were estimated over the range J = 0–816. In this case I experimented with one other time-saving measure – summing over J = 0, M, $2M$, $3M$, etc., with multiplication of the final sum by M. (The motivation for this procedure is the observation that for homonuclear molecules having zero nuclear spin, alternate levels are rigorously absent from the sum.)

The results of the calculations for the Morse potentials are compared with RR/HO and rigid-rotor/Morse oscillator (RR/MO) values as functions of T in fig. 1. (Note that the latter is *not* the same as the full rotation–vibration calculation for the Morse potentials in my tests.) As expected the RR/HO results are poorer than the RR/MO values, since the latter correctly

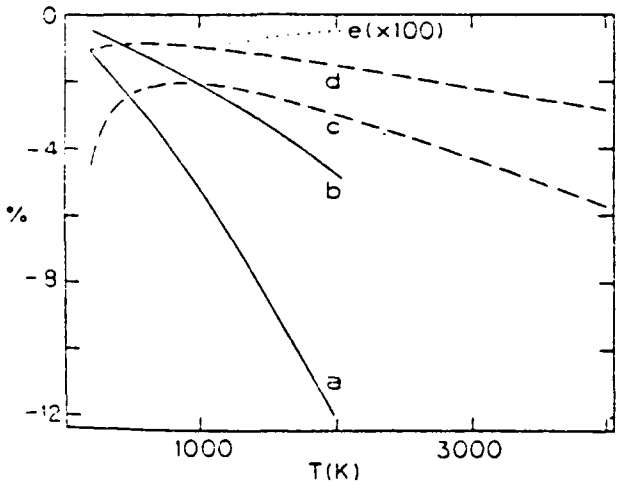

Fig. 1. Percent error in various estimates of q_{vr} for I_2 (a, b, e) and O_2 (c, d) as functions of T. Curves (a) and (c) are for the RR/HO model, curves (b) and (d) for the RR/MO model. Curve (e) shows the percent error (×100) in the "exact" calculation for M = 5.

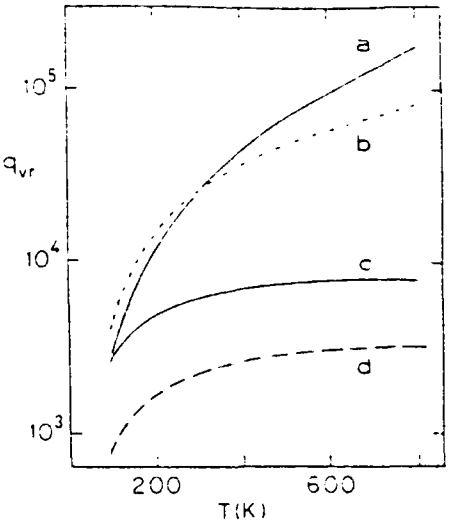

Fig. 2. Comparison of partition functions for Ar_2 calculated using the RR/HO model [curve (a)], the RR/MO model (b), and the "exact" result (c). Also shown is the metastable contribution to the last of these (d).

take into account the vibrational anharmonicity. Both models fall increasingly below the exact results as T increases; this is attributable to the omission of the vibration–rotation interaction, since q_r for the RR model is proportional to the inverse of the rotational constant B_v, and the latter decreases with increasing v. The reason for the anomalously low values at low T for the "O_2" tests are (1) the use of B_e instead of B_0 in q_r, and (2) a 5 cm^{-1} error in the zero-point energy in the case of the RR/HO calculation. With these changes the results for both molecules would be much closer to exact at T = 200 K.

At temperatures much higher than those covered in fig. 1, both the RR/HO and RR/MO results must eventually exceed the exact q_{vr}. This is evident in fig. 2, where the comparison is given for the Ar_2 test case. At high T the exact value approaches a constant, in recognition of the existence of a finite number of bound and metastable levels. Both the RR/HO and RR/MO values continue to increase with T due to the direct proportionality on T in q_r for the RR model, however, the RR/MO model correctly includes the finite vibrational spectrum, so is somewhat better at high T. Of course it is precisely the region where the "exact" q_{vr} is leveling off that the continuum contributions become important [3], so the latter should really be included for a proper comparison (which,

however, is beyond the scope of this work).

As shown by curve (e) in fig. 1, the inclusion of only every fifth J in the rotational sum for I_2 leads to an error which is probably negligible everywhere, except possibly at low T. Use of $M = 2$ gave about a factor of four smaller error. The error, however, is systematic, and it is clearly a function of the particular molecule and temperature in question, being smaller for large μ and T. In any event it appears that the calculations are already efficient enough to permit evaluation of the full rotational sum in most cases, without excessive use of CPU time.

4. Conclusion

The Morse oscillator is a workhorse in diatomic calculations requiring a "realistic" potential. Indeed it has been used previously in test calculations of partition functions (see, e.g. refs. [19–22]). However, many such studies have treated just the vibrational partition function rather than the full rotation–vibration partition function, when in fact it is the latter that is needed for thermodynamic applications. The scheme I have described is applicable to *any* potential at *any* temperature. Of course it *does* require a potential and will obviously be limited by uncertainties in the potential. And it is of limited use in cases such as that of Ar_2 treated here, where the continuum contributions to q_{vJ} are needed to account for the total "Ar_2" (which may be negative!) in equilibrium with Ar atoms. However, even in cases such as this, it can be used to assess total concentrations of bound and metastable molecules, or concentrations in selected bound or metastable (v, J) levels.

Originally I developed the present semiclassical method for the purpose of testing partition functions calculated by the classical method [3,23]. However, in the course of conducting the present calculations, it has become clear to me that the method has value in its own right. Since most of the computational time is invested in the determination of the eigenvalues, one can evaluate q_{vJ} at a large number of temperatures in a single pass, at little additional expense. (Sums including E and E^2 under the summation sign can also be evaluated directly rather than estimated from temperature derivatives.) For the classical partition function, on the other hand, a completely new (albeit simple and fast) calculation is required at each T.

To the best of my knowledge, the simple method I have described here has not previously been described in the literature and is not known or used by thermodynamicists. However, since completing the present calculations, I have discovered that a very similar procedure *was* used 35 years ago by Woolley et al. [24], to estimate contributions from high (v, J) levels to partition functions of H_2 at high temperatures. These authors even used an RKR-like procedure to determine the width of their rotationless potential as a function of v. However, their work was completed before the advent of modern computers, and it appears the authors did not recognize either the great accuracy of the semiclassical phase integral or the efficiency with which it can be evaluated using the Gauss–Mehler quadrature. Accordingly their method seems to have been ignored in subsequent work. Now it is clear that techniques based on the semiclassical phase integral can be useful in any calculation where levels near dissociation are important, since they can yield directly the number of bound and metastable levels and their energy range (tables 1 and 2), as well as their contributions to q_{vJ} (fig. 2).

Acknowledgement

This work was supported in part by the Air Force Office of Scientific Research and the Office of Naval Research.

References

[1] T.L. Hill, An introduction to statistical thermodynamics (Addison-Wesley, Reading, 1960).
[2] K.S. Pitzer and L. Brewer, Thermodynamics (McGraw-Hill, New York, 1961). [Revised from original by G.N. Lewis and M. Randall].
[3] F.H. Mies and P.S. Julienne, J. Chem. Phys. 77 (1982) 6162.
[4] G. Herzberg, Spectra of diatomic molecules (Van Nostrand, Princeton, 1950).
[5] J.L. Dunham, Phys. Rev. 41 (1932) 721.
[6] R.J. Le Roy and W.-H. Lam, Chem. Phys. Letters 71 (1980) 544.
[7] J.W. Tromp and R.J. Le Roy, Can. J. Phys. 60 (1982) 26.
[8] J. Tellinghuisen, J. Chem. Phys. 78 (1983) 2374.

[9] J.W. Tromp and R.J.Le Roy, to be published.
[10] A.W. Mantz, J.K.G. Watson, K.N. Rao, D.L. Albritton, A.L. Schmeltekopf and R.N. Zare, J. Mol. Spectry. 39 (1971) 180.
[11] J.W. Cooley, Math. Comp. 15 (1961) 363.
[12] R.N. Zare and J.K. Cashion, Lawrence Berkeley Laboratory Report UCRL 10881 (1963).
[13] J.K. Cashion, J. Chem. Phys. 39 (1963) 1872.
[14] R.N. Zare, J. Chem. Phys. 40 (1964) 1934.
[15] J. Tellinghuisen, J. Phys. B13 (1980) 4781.
[16] J. Tellinghuisen, Chem. Phys. Letters 18 (1973) 544.
[17] J. Tellinghuisen, J. Mol. Spectry. 44 (1972) 194.
[18] Z. Kopal, Numerical analysis (Chapman and Hall, London, 1961).
[19] R.W. Crecely and D.J. Wilson, J. Chem. Phys. 41 (1964) 1564.
[20] T. Ishida, J. Chem. Phys. 61 (1974) 3009.
[21] V.T. Amorebieta and A.J. Colussi, Chem. Phys. Letters 82 (1981) 530.
[22] V.T. Amorebieta and A.J. Colussi, Chem. Phys. Letters 98 (1983) 315.
[23] F.H. Mies and P.S. Julienne, to be published.
[24] H.W. Wooley, R.B. Scott and F.G. Brickwedde, J. Res. Natl. Bur. Std. 41 (1948) 379.

$B \rightarrow X$ transition in $^{136}Xe\ ^{19}F$

Patricia C. Tellinghuisen and Joel Tellinghuisen
Department of Chemistry, Vanderbilt University, Nashville, Tennessee 37235

(Received 2 August 1983; accepted for publication 7 September 1983)

The $B \rightarrow X$ emission spectrum is analyzed for the single isotopomer $^{136}Xe\ ^{19}F$. Thirteen v'-v'' bands spanning $v' = 0$–4 and $v'' = 0$–5 have been rotationally analyzed. The analysis yields greatly improved spectroscopic constants, permitting precise identification of most of the features in the XeF laser spectrum. No evidence is found for $C \rightarrow X$ emission in the normal sense. However, it is possible that several previously unassigned features, including one or more reported laser lines, constitute $C \rightarrow X$ emission enabled through intensity borrowing from B-X by B-C perturbative mixing.

PACS numbers: 33.20.Kf, 33.70. – w, 35.20.Pa, 35.20.Sd

The diatomic rare gas halides burst into prominence eight years ago as lasants in a new class of excimer laser. At that time these molecules were virtually unknown spectroscopically. Their essential properties were rapidly determined from theoretical and experimental studies.[1] In fact, most of the lasing $B \rightarrow X$ transitions turned out to be spectroscopically "simple," the only structure in their bound-free emission spectra being Franck–Condon structure. Only in the cases of XeF, XeCl, and XeBr has discrete structure been observed. (In the last case the discrete structure is just barely discernible and has not yet been analyzed.[2])

The most interesting RgX molecule from the spectroscopic standpoint (and one of the more interesting high-power laser candidates) is XeF. The $B \rightarrow X$ and $D \rightarrow X$ transitions in XeF were analyzed in emission[3–5] and absorption[6] shortly after the XeF laser was reported. Nozzle-beam studies[7] corroborated the sketchy rotational analysis of B-X in the emission work and gave additional information about high v' and low v'' levels. Very recently the third ion-pair excited state, $C(3/2)$, has been characterized through the weak $C \leftarrow X$ transition.[8,9] However, the spectroscopic description of the B-X transition remains marginal for the identification of the lasing transitions, mainly because of ambiguities stemming from isotope effects in the spectrum of "natural" XeF, which contains predominantly ^{129}Xe (26%), ^{131}Xe (21%), and ^{132}Xe (27%). To remedy this situation we have been studying the emission spectrum of the single XeF isotopomer: $^{136}Xe\ ^{19}F$. This work is now sufficiently completed to permit reliable assignment of most of the features in the laser spectrum.

The emission spectrum was photographed in the region 3300–3600 Å, using equipment and procedures similar to those described previously.[10–12] The Tesla discharge sources were charged with 1–1.5 Torr SF_6, 2–3 Torr ^{136}Xe (Mound Laboratory, 95.2% isotopic purity), and 140–170 Torr Ar. (These pressures of SF_6 and Xe, with 400–600 Torr Ar, were found to give optimum intensity; however, the lower Ar pressure was employed to keep line broadening negligible.) The photographic plates had a reciprocal dispersion of 1.35 Å/mm and a resolving power greater than 200 000. The spectra were calibrated with Fe atomic lines. We estimate that sharp, unblended lines are measured with an absolute accuracy of $\pm 0.02\ cm^{-1}$, which is comparable to the standard deviations obtained in our least-squares fits, described below.

To date we have rotationally analyzed 13 v'-v'' bands spanning $v' = 0$–4 and $v'' = 0$–5. In some cases (particularly the strong bands from $v' = 0$) we are able to extend the assignments to $N'' > 70$. However, when the data are fitted to the Hamiltonians given for the B and X states in Ref. 4, the quality of the fit deteriorates rapidly for $N > 45$. This problem was noted earlier and is still under investigation. In the meantime, to obtain optimal constants for the low-N lines, we have fitted only the assignments for $N < 41$. Results of the

TABLE I. Spectroscopic constants from band-by-band rotational analysis of $B \rightarrow X$ spectrum of $^{136}Xe\ ^{19}F$. All quantities are given in cm^{-1}. Constants are as defined in Ref. 5.

v'-v''	ν_0	B'	B''	$D'' \times 10^7$	δ	α	$b \times 10^{10}$	σ
1-2[a]	28 773.877(10)	0.144 70(6)	0.175 10(7)	9.63(17)	1.868 51	− 0.083 19	− 2.45	0.035
2-1	29 259.121(8)	0.143 77(4)	0.181 62(5)	7.78(13)	1.808 26	− 0.036 60	− 4.32	0.023
1-1	28 956.942(9)	0.144 54(5)	0.181 63(6)	7.97(14)	1.787 88	− 0.017 80	− 3.47	0.031
0-5	28 055.618(34)	0.145 29(15)	0.146 79(17)	18.72(43)	1.737 71	0.024 67	− 4.18	0.042
0-4	28 169.789(13)	0.145 28(9)	0.157 97(10)	15.25(20)	1.814 47	− 0.051 09	− 3.23	0.029
0-1	28 651.772(8)	0.145 24(5)	0.181 59(5)	7.98(14)	1.830 61	− 0.047 29	− 0.84	0.029
0-3	28 307.600(8)	0.145 31(4)	0.167 17(5)	11.96(13)	1.832 37	− 0.049 28	− 5.06	0.022
0-2	28 468.711(12)	0.145 20(5)	0.174 84(6)	9.61(16)	1.877 15	− 0.079 82	− 4.54	0.029
4-0	30 058.082(10)	0.142 19(7)	0.187 39(8)	6.77(19)	1.787 50	− 0.049 01	5.88	0.036
4-1	29 854.485(9)	0.142 37(6)	0.181 72(6)	7.90(16)	1.865 34	− 0.111 15	10.37	0.030
2-0	29 462.708(14)	0.143 77(7)	0.187 40(8)	6.58(22)	1.803 99	− 0.033 91	− 8.77	0.034
4-4	29 372.448(33)	0.142 26(7)	0.158 04(9)	15.86(31)	1.778 29	0.057 86	1.65	0.030
3-3	29 214.100(18)	0.142 70(7)	0.166 74(10)	11.28(28)	1.813 13	− 0.047 67	0.44	0.031

[a] Analyzed in Ref. 5. Present results indicate a probable calibration error of $-0.81\ cm^{-1}$ in the data in Table I of Ref. 5.

band-by-band fits are summarized in Table I, in which the constants are as defined in Refs. 4 and 5. The constants for each band represent typically 20–25 assigned lines in each of the four branches (P_1, P_2, R_1, R_2), although the assignments are somewhat sparser for those bands involving $v'' = 4$ and 5, in which the rotational structure is very congested.

To obtain the usual spectroscopic expansion coefficients for the B-X band system, we proceeded as follows. The estimated band origins from Ref. 5 were augmented by the band origins from Table I (heavily weighted in accord with their much greater precision) and were fitted directly to the usual double polynomials in $[\rho(v' + 1/2)]$ and $[\rho(v'' + 1/2)]$, where ρ is the isotopic factor, related to the reduced masses by $\rho = (\mu_r/u)^{1/2}$. We take ^{136}XeF to be the reference molecule (μ_r). The data from Ref. 5 were taken to represent the hypothetical "average" molecule, $^{131.3}$XeF, for which $\rho = 1.00215$. (Attempts to give the various features more specific isotopic assignments actually gave poorer variances, hence were abandoned.) To fit these data adequately, it was necessary to use seven vibrational parameters for the X state (cf. five in Ref. 5). This is indicative of the anomalous nature of the XeF ground state, since the number of vibrational parameters is only three less than the number of levels represented (0–9). For the B state three parameters gave a slightly better fit than two, with the data spanning $v' = 0$–15.

To obtain the rotational and spin-splitting constants, we employed a correlated fit of the relevant results in Table I and their associated variance-covariance matrices, using methods like those outlined by Albritton *et al.*[13] and used previously by us.[14] Here, again we found that the X-state rotational constants were not well overdetermined, as five parameters were needed to represent the six observed levels 0–5. (The five expansion parameters, however, were better than a direct fit to the six individual B_v'' values, and they gave virtually identical results.) Two parameters were adequate for B_v' and three for D_v'', while three were required for both $\delta B_v'$ and $\alpha B_v''$ [also expressed as polynomials in $(v' + 1/2)$ and $(v'' + 1/2)$]. The "extra" centrifugal distortion parameter b, which was introduced in Ref. 5, showed stronger correlation with v' than with v'', so was expressed as a linear function of $(v' + 1/2)$. These results are summarized together with the vibrational parameters in Table II. It is worth noting that our results are similar to, but not completely consistent with, the only other rotational analysis of this system, that of Ref. 7. For example, the estimate of R_e'' in the latter work was 2.321(2) Å.

Although the constants in Table II are strictly valid for only the ^{136}XeF isotopomer, we expect them to be applicable to the other isotopomers as well, at least to a good approximation. To use them in this way, one replaces $(v + 1/2)$ by $\rho(v + 1/2)$ everywhere, and κ [$\approx J(J + 1)$ or $N(N + 1)$, see Refs. 4 and 5] by $\rho^2\kappa$, where $\rho = 1.00332$ for ^{129}XeF, 1.00234 for ^{131}XeF, 1.00186 for ^{132}XeF, and 1.00092 for ^{134}XeF. We assume that the spin-splitting parameters δ and α show no specific isotope dependence. Since these parameters are given in Table II in the coupled forms $\delta B_v'$ and $\alpha B_v''$, in which they were determined in the fits, we have extracted and presented in Table III the explicit values. It should be noted that these constants are much less precisely determined than are

TABLE II. Recommended spectroscopic parameters (cm^{-1}) for the B–X transition in ^{136}Xe^{19}F.[a,b]

	X	B
T_e	0	28 811.61(14)
$c_{e1}(\omega_e)$	226.193(523)	308.176(14)
$c_{e2}(-\omega_e x_e)$	13.592(629)	1.506(5)
c_{e3}	2.410 8	1.37×10^{-3}
c_{e4}	$-8.372\,2 \times 10^{-4}$	
c_{e5}	$1.412\,4 \times 10^{-4}$	
c_{e6}	$1.193\,8 \times 10^{-5}$	
c_{e7}	$4.033\,2 \times 10^{-6}$	
$c_{v0}(B_e)$	0.190 052(71)	0.145 674(50)
$c_{v1}(-\alpha_e)$	$-5.016\,9(657) \times 10^{-4}$	$7.565(24) \times 10^{-4}$
c_{v2}	$-4.083\,8 \times 10^{-4}$	
c_{v3}	$1.352\,2 \times 10^{-5}$	
c_{v4}	$-6.056\,0 \times 10^{-6}$	
R_e(Å)	2.306 9(4)	2.634 9(4)
$c_{\alpha 0}$[c]	$-1.145(262) \times 10^{-2}$	0.268 56(261)
$c_{\alpha 1}$[c]	1.833×10^{-3}	$-1.884\,0 \times 10^{-3}$
$c_{\alpha 2}$[c]	3.885×10^{-4}	$2.005\,2 \times 10^{-4}$
$c_{d0}(D_e)$	$6.42(36) \times 10^{-7}$	
c_{d1}	4.12×10^{-8}	
c_{d2}	3.41×10^{-8}	
b_0		5.2×10^{-10}
b_1		1.5×10^{-10}

[a] The given quantities are coefficients of polynomials in $(v' + 1/2)$, with numerical subscripts indicating the power of the argument. Where given, the figures in parentheses represent standard errors, in terms of final digits.

[b] Vibrational parameters valid for $v' = 0$–15, $v'' = 0$–9; rotational parameters valid for $v' = 0$–4, $v'' = 0$–5. The parameters are given to sufficient precision to permit recalculation of original results within experimental error.

[c] Quantities not given (e.g., D_v' and H_v'') remain as estimated in Table V of Ref. 5.

[d] Coefficients of polynomials for $\alpha B_v''$ and $\delta B_v'$, respectively.

B_v' and B_v''. In fact, δ and α show very high negative correlation, so that the quantity which is well determined is the sum $\delta B_v' + \alpha B_v''$.

The strongest features in the XeF laser spectrum are groups of lines near 3511 and 3532 Å,[4,15] with the former predominating under some circumstances and the latter under other.[16–18] The present results solidify the earlier, more tentative assignment of these features.[4] For example, we show in Fig. 1 the high-resolution spectrum near 3511 Å, with calculated rotational assignments for the 1–4 and 0–2 bands. Even under the present very high resolution, the rotational structure in this region is only marginally resolved. In a high-pressure laser operating on "natural" XeF, isotope shifts and pressure broadening produce further blurring of this structure.[4]

TABLE III. Spin-splitting parameters for X and B states of XeF.

v	α	δ
0	−0.0567	1.8415
1	0.0527	1.8353
2	0.0531	1.8263
3	0.0586	1.8144
4	0.0701	1.7995
5	0.0894	1.7817
6	0.1198	

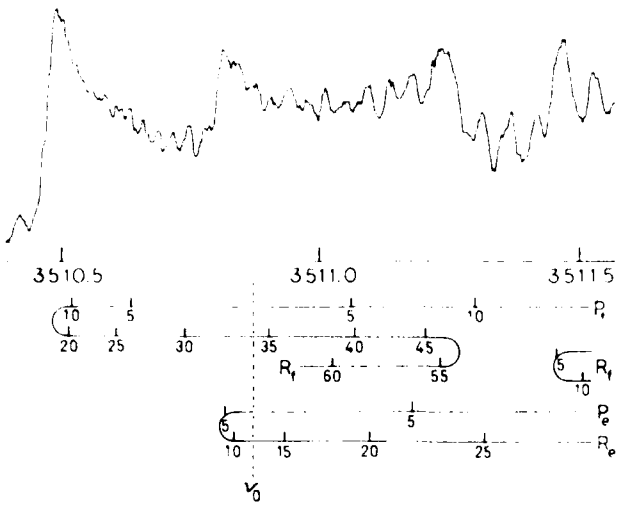

FIG. 1. Densitometer tracing of the emission spectrum of ^{136}XeF near 3511 Å, showing rotational branch structure in the 1–4 band. Also shown (to right) is the R_f head in the 0–2 band.

In their recent analysis of the $C \rightarrow X$ spectrum, Helm *et al.*[8,9] have located the C state near $R_e = 2.45$ Å and 28023 cm^{-1}, or about 0.2 Å to smaller R and 789 cm^{-1} below the B state. They have also suggested that for thermally equilibrated B and C states, the $C \rightarrow X$ emission could account for as much as 35% of the total UV emission. We have looked for $C \rightarrow X$ bands in our spectra and have found no evidence of them. In this regard, we note that the strongest $C \rightarrow X$ bands should be 0–1 and 0–2, which are calculated to lie near 27 883 and 27 700 cm^{-1}, respectively. This is in the red wings of the $B \rightarrow X$ system, where only very weak emission occurs from $v' = 0$ to $v'' \sim 7$, so $C \rightarrow X$ emission should be easily discerned. Since our single isotope sources were operated at low pressures, we also reexamined the Sandia spectra,[4] which were recorded at $P \sim 2$ atm. Again we found no evidence of the predicted $C \rightarrow X$ bands. From this result we conclude that the $C \rightarrow X$ system must be at least a factor of ~ 30 weaker than suggested in Refs. 8 and 9.

The analysis of the C state also permits us to predict perturbations in the $B \rightarrow X$ spectrum. For low v_B, levels $v_C = v_B + 2$ lie somewhat below v_B, catching up near $v_B = 3$. Also, because the rotational constants are larger for C than for B, the rotational levels of C overhaul those of B from below, so that perturbations should occur for rotational quantum numbers as low as ~ 20 in $v_B = 3$, or as high as ~ 70 in $v_B = 0$. So far we have not been able to identify such perturbations, although the search has not been exhaustive. However, we *do* think it likely that the previously mentioned problems with the fit Hamiltonian are due to an anomalous centrifugal distortion of the B state due to interaction with the C state. It is also possible that some of the previously unassigned features[4] may in fact be $C \rightarrow X$ emission from C-state levels that borrow intensity from $B \rightarrow X$ through B-C perturbative mixing. In this regard it is interesting to note that one of the weaker laser lines reported by Shimauchi *et al.*[15] (at 3502.475 Å) coincides with one of the strong, unassigned features in Ref. 4. Thus it is conceivable that the $C \rightarrow X$ transition has even been made to lase, though in a rather special way! We are continuing work on these problems.

This work was supported by DARPA and ONR.

[1] E. W. McDaniel and W. L. Nighan, eds., *Applied Atomic Collision Physics: Vol. 3-Gas Lasers* (Academic, New York, 1982).
[2] K. S. Viswanathan and J. Tellinghuisen (unpublished).
[3] J. Tellinghuisen, G. C. Tisone, J. M. Hoffman, and A. K. Hays, J. Chem. Phys. **64**, 4796 (1976).
[4] J. Tellinghuisen, P. C. Tellinghuisen, G. C. Tisone, J. M. Hoffman, and A. K. Hays, J. Chem. Phys. **68**, 5177 (1978).
[5] P. C. Tellinghuisen, J. Tellinghuisen, J. A. Coxon, J. E. Velazco, and D. W. Setser, J. Chem. Phys. **68**, 5187 (1978).
[6] A. L. Smith and P. C. Kobrinsky, J. Mol. Spectrosc. **69**, 1 (1978).
[7] D. L. Monts, L. M. Ziurys, S. M. Beck, M. G. Liverman, and R. E. Smalley, J. Chem. Phys. **71**, 4057 (1979).
[8] H. Helm, D. L. Huestis, and D. C. Lorents, in *Excimer Lasers-1983*, edited by C. K. Rhodes, H. Egger, and H. Pummer (AIP, New York, 1983), Vol. 100, p. 216.
[9] H. Helm, D. L. Huestis, and C. D. Lorents, J. Chem. Phys. **79**, 3220 (1983).
[10] M. R. McKeever, A. Sur, A. K. Hui, and J. Tellinghuisen, Rev. Sci. Instrum. **50**, 1136 (1979).
[11] A. Sur, A. K. Hui, and J. Tellinghuisen, J. Mol. Spectrosc. **74**, 465 (1979).
[12] J. Tellinghuisen and J. G. Ashmore, Appl. Phys. Lett. **40**, 867 (1982).
[13] D. L. Albritton, A. L. Schmeltekopf, and R. N. Zare, in *Molecular Spectroscopy: Modern Research*, edited by K. Narahari Rao (Academic, New York, 1976), Vol. II, p. 1.
[14] J. Wei and J. Tellinghuisen, J. Mol. Spectrosc. **50**, 317 (1974).
[15] M. Shimauchi, S. Karasawa, and T. Miura, Jpn. J. Appl. Phys. **17**, 527 (1978).
[16] R. W. Tuxworth, M. Lawton, and M. J. Shaw, J. Phys. D **13**, 135 (1980).
[17] V. Y. Baranov, V. M. Borisov, Y. Y. Stepanov, and O. B. Khristoforov, Sov. J. Quantum Electron. **10**, 794 (1980).
[18] W. E. Ernst and F. K. Tittel, J. Appl. Phys. **51**, 2432 (1980).

0018–1536/84/1700–0289$02.60

Diatomic Partition Functions from Classical and Semiclassical Phase Integrals

JOEL TELLINGHUISEN

Department of Chemistry, Vanderbilt University, Nashville, Tennessee, 37235

Received September 23, 1983; Accepted December 31, 1983

ABSTRACT

Two methods for calculating diatomic partition functions directly from potential curves are examined with regard to their computational efficiency and accuracy. The first utilizes semiclassical phase integrals to estimate the rotation–vibration eigenvalues and may be considered exact. The second method entails numerical integration of the classical phase integral. The two methods are compared in test calculations of the bound and metastable contributions to the partition functions q_{vr} for Ar_2 and HgBr. These calculations show that the classical method, which is typically one to two orders of magnitude faster than the semiclassical method, gives results for the bound contributions to q_{vr} within 1% of exact when kT is at least twice the vibrational energy. For the metastable contributions, two alternative modifications of the classical expression perform less well, and it appears that these contributions can best be estimated by the semiclassical method.

The calculations for HgBr employ the latest spectroscopic constants for this molecule. The resulting values of q_{vr} are represented within 0.2% over the range 200–3000 K by an empirical expression containing six parameters, with the latter determined by the method of least squares.

Index Entries: Partition functions, of diatomic molecules; classical phase integrals, for diatomic partition functions; semiclassical phase integrals, for diatomic partition functions; HgBr, diatomic partition functions for; diatomic partition functions.

INTRODUCTION

Although Leo Brewer is very much "the Compleate Scientiste," he has always been, first and foremost, a thermodynamicist. Yet in the late 60s, when I was a member of his research group, there was a strong spectroscopic thrust to his research efforts, centered mainly around work on radiative lifetimes and the characterization of species isolated in low-temperature matrices. The problems that occupied most of my time and effort and became my thesis project were not directly concerned with thermodynamics or even with high temperatures. Rather, they involved the spectroscopy and photophysics of the I_2 molecule, and they developed almost "involuntarily," as a spinoff of an unexpected v'-dependence in decay rates measured on exciting I_2 to the B state at various wavelengths. (I_2 was originally to have been the simple test case for checking out the lifetime equipment prior to conducting experiments on high-temperature diatomics; it ended up as at least a major component of ~10 PhD theses and publications from Brewer's group.) In any event, with my preoccupation with I_2 (which continues today), I must confess that I completed my tenure with Leo without ever removing an uneasy feeling from the pit of my stomach . . . the fear that I didn't really understand thermodynamics!

Years of teaching thermo and statistical mechanics have done much to remedy that malaise. Now, although I am not active in thermodynamics on the research level, I feel at least conversant with the subject. Recently I have come to reconsider one of Leo's favorite thermodynamic aphorisms: "Thermodynamics doesn't care what you call a material—atoms, molecules, or whatever; as long as you treat the system consistently, you will obtain correct results." When I first heard him say this, I had a gut understanding that the truth of this statement was wrapped up in those fudge factors we know as activity and fugacity coefficients. But I think I might have been hard pressed to verify the point through numerical calculations. Now I believe I can do the latter, at least for the simplest kind of system—gaseous dimers in equilibrium with their parent atoms.

Although thermodynamics doesn't care about the formal definition of a system, the thermodynamicist can simplify his numerical calculations by choosing a definition which makes the system as close to "ideal" as possible. For example, we can call a container of xenon gas "Xe" or "Xe_2"; but under most conditions (except possibly at very low temperature and high pressure) the latter definition will show deviations roughly a factor of two from ideal in PVT behavior, and will require anomalous fugacity coefficients far from unity. On the other hand, by defining the system as a mixture of Xe and Xe_2 in equilibrium at all times, we can force the thermodynamics toward ideality. If we are careful how we define "Xe" and "Xe_2" in this system, we can be sure that any further deviations from ideality can be attributed to "polyatomic" contributions (e.g., Xe_3, Xe + Xe_2, Xe + Xe + Xe, Xe_2 + Xe_2, Xe_4, etc.). Then, in principle at

least, we could redefine our system once again to include such species, and thereby force the system into still closer compliance with ideality.

In a recent paper (*1*) Mies and Julienne have shown very clearly how the partitioning of the system, dimers ↔ atoms, is to be carried out on a statistical mechanical level, in order to achieve the desired rigorously ideal behavior (neglecting higher-order interactions, of course, but including atom–atom collisions). Among their recommendations were the following: (1) To achieve ideal *PVT* behavior for this system, one should include the molecular continuum and metastable levels in the partition function q_{vr} for the dimer. (2) The safest procedure for evaluating q_{vr} is to begin with the potential curve or curves which define the molecular states of significance. (3) At high temperatures the classical method is both very accurate and by far the easiest procedure for evaluating q_{vr}. It is worth noting (as Mies and Julienne do) that similar recommendations were put forward long ago [e.g., refs. (*3*) and (*4*)], but were never fully developed. It should also be mentioned that for weakly attracting species such as the rare gases, this approach may lead to *negative* concentrations of "molecules" over much of the temperature range! This is because excluded volume effects dominate and contribute negatively to the continuum part of q_{vr}.

I can add nothing to the formal treatment by Mies and Julienne and can only recommend that their paper receive close scrutiny. However, I can offer some information and suggestions on the mechanics of calculating the molecular partition functions. In a recent paper I described a very efficient computational procedure for evaluating the "exact" bound and metastable contributions to the diatomic partition function for any potential at any temperature (*5*). This method utilizes semiclassical phase integrals to obtain the eigenvalues. Its accuracy and efficiency are attributable to the following observations: (1) For "realistic" diatomic potentials, the first-order semiclassical eigenvalues are very close to the quantum mechanical eigenvalues (typically within 1 cm^{-1}); for the RKR potentials commonly used by diatomic spectroscopists, they are exact by definition. (2) The semiclassical eigenvalues can be evaluated very quickly and accurately by means of the Gauss-Mehler quadrature (*6*), coupled with interpolation. As a consequence, partition functions can be calculated by this method about as quickly as through the usual sum over states using spectroscopic constants to calculate the latter, and without certain problems concerning the range of validity of these spectroscopic constants (*5*).

In spite of its accuracy and efficiency, the semiclassical procedure is still slower and more intricate to code for machine computations than is the classical method. The latter is also particularly easy to apply when the molecular continuum is included in the phase space of the dimers (*1*, *2*). In the present paper I have carried out numerical calculations designed to examine the validity of the classical method, using the semiclassical method as my benchmark. The test cases are a weakly

bound dimer (Ar_2) approximated by a 6–12 potential, and a more realistic "high-temperature" species (HgBr) having an RKR-based potential defined by recent spectroscopic work. These calculations indicate that the classical method is virtually exact at high temperatures and surprisingly accurate even at temperatures low enough to make it suspect (i.e., where the vibrational energy interval is roughly equal to kT). Although the calculations focus on just the bound and metastable contributions to q_{vr}, the near exact performance of the classical method for these parts makes it plausible that similar reliability will hold for the continuum region, in agreement with the suggestions of Mies and Julienne (*1*, *2*).

THEORY

The usual starting approximation for evaluating the rotation–vibration partition function q_{vr} of a diatomic molecule is the rigid rotor/harmonic oscillator (RR/HO) model (*7*). At not-too-high temperatures the RR/HO partition function may be corrected for effects of anharmonicity, rotation-vibration interaction and centrifugal distortion (*8*). With increasing T these approximations must eventually fail, and the only safe procedure is the direct sum over states of the Boltzmann factors. In the usual implementation of this method, one uses spectroscopic constants to represent the energies $E(v, J)$ as functions of v and J, the vibrational and rotational quantum numbers. Whereas this procedure is computationally easy to perform using modern computers, one must nevertheless exercise caution in extrapolating the expressions for the spectroscopic constants beyond their range of validity, i.e., the range of the spectroscopic observations. It is for this reason that methods that focus on the molecular potential rather than the spectroscopic constants are preferred at high T, because the potential can be extrapolated to dissociation more easily than can the spectroscopic constants. [However, the recently developed methods that represent the spectroscopic constants by expressions using the dissociation limit as reference (*9–11*) make the use of spectroscopic constants much more straightforward for levels near dissociation.]

Apart from fine effects related to electron spin interactions, which for thermodynamics calculations can usually be handled through a simple degeneracy factor, the eigenvalues $E(v, J)$ for a given electronic state of a diatomic molecule are the solutions of the Schrödinger equation for the effective potential.

$$U_J(R) = U_0(R) + \beta J(J + 1)/R^2 \qquad (1)$$

where the constant β is inversely proportional to the molecular reduced mass μ. (In cm^{-1} units, $\beta = B_e R_e^2$, where B_e and R_e are the equilibrium rotational constant and internuclear distance, respectively.) Thus if the rotationless potential $U_0(R)$ is known, one can systematically solve for all the eigenvalues of each effective potential $U_J(R)$, $J = 0, 1, 2, \ldots$ To do so

by quantum mechanical methods, however, is tedious and expensive in CPU time, except for very light molecules or shallow potentials. As an alternative, I have employed the semiclassical phase integral (5),

$$h(v + 1/2) = (8\mu)^{1/2} \int_{R_1}^{R_2} [E - U_J(R)]^{1/2} dR \qquad (2)$$

where h is Planck's constant and R_1 and R_2 are the classical turning points for energy E. The method I have devised based on this approach is very efficient; in test calculations I was able to evaluate 5×10^4 eigenvalues and ~10 partition functions in several minutes of CPU time on a DEC-1099 (not a "supercomputer").

Assuming that the potential $U_0(R)$ represents the ground electronic state of the diatomic and there are no other low-lying electronic states, the molecular partition function is just

$$q_{vr} = \sum_{J,v} (2J + 1) e^{-E(v, J)/kT} \qquad (3)$$

The energy levels are designated as bound, metastable, or continuum levels, depending on the relationship of $E(v, J)$ to the effective potential $U_J(R)$. For reference, I show in Fig. 1 effective potentials for $J = 0$, 200, 350, and 500 for a Morse curve approximating HgBr (see below). All levels having $E < \mathfrak{D}_e$ are bound. All levels lying above the rotational barrier $E_{b,J}$ for that J belong to the continuum. Those levels inside the well for which $\mathfrak{D}_e \le E \le E_{b,J}$ are designated as metastable. Note that for $J > 350$ in Fig. 1, only metastable and continuum levels exist, whereas for $J > 500$ only continuum levels occur. In the present test calculations I am concerned with only the bound and metastable contributions to q_{vr}, which always dominate at sufficiently low T. For the continuum contributions one must be careful to include just the "molecular" part of the continuum, i.e., to exclude contributions from colliding noninteracting (ideal) atoms (1, 2, 12). (Note that for noninteracting atoms, $U_0 = 0$, but $U_J \neq 0$ for $J \neq 0$).

The classical partition function q_{cl} is given by the classical phase integral (7).

$$q_{cl} = h^{-n} \int exp[-H_{cl}(q, p)/kT] dq_1 dp_1 \ldots dq_n dp_n \qquad (4)$$

where n is the number of degrees of freedom, and q_i and p_i are conjugate coordinate and momentum variables. In the present case, $n = 3$, and we can conveniently express the element of volume in phase space in Cartesian or spherical coordinates:

$$d\tau = dq_1 dp_1 \ldots dq_3 dp_3 = dx dp_x dy dp_y dz dp_z = dR dp_R d\theta dp_\theta d\varphi dp_\varphi \qquad (5)$$

The classical Hamiltonian is the sum of kinetic and potential energies. Since the latter is a function of internuclear separation only, it is more appropriate to use spherical coordinates.

$$H_{cl} = (1/2\mu)[p_R^2 + (p_\varphi/R)^2 + (p_\theta/R \sin\theta)^2] + U_0(R) \qquad (6)$$

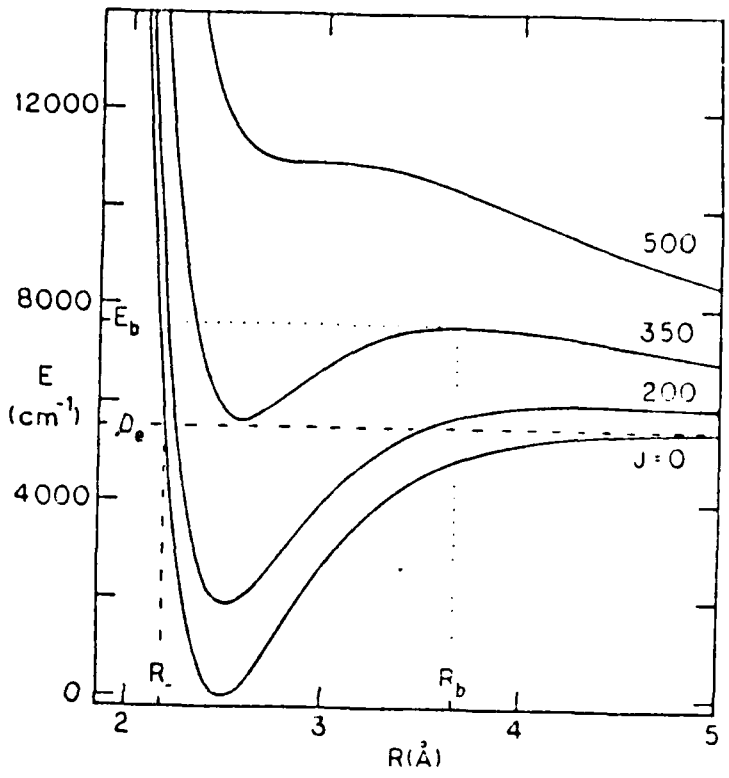

Fig. 1. Effective potentials, $U_J(R)$, for HgBr at selected values of the rotational quantum number J. Also shown are the quantities $\mathfrak{D}_e$ and R_- for the rotationless curve, and the location of the barrier (R_b, E_b) for $J = 350$.

For the bound part of q_{cl} we must include just that part of phase space that restricts the particle to be within the well. This we do by limiting the total kinetic energy to the value, $\mathfrak{D}_e - U_0(R)$. For this purpose it is only the total magnitude of the momentum that is important, and it is convenient to rewrite Eqs. (5) and (6) as

$$d\tau = (4\pi p^2 dp)(4\pi R^2 dR) \qquad (7)$$

and

$$H_{cl} = (p^2/2\mu) + U_0(R) \qquad (8)$$

Now the momentum integral in Eq. (4) is limited to the range, $-p_{max}(R) \le p \le p_{max}(R)$, where

$$p^2_{max} = 2\mu[\mathfrak{D}_e - U_0(R)] \qquad (9)$$

Correspondingly, the coordinate integral is limited to the range of R where $\mathfrak{T}_e \geq U_0(R)$, $R_- \leq R \leq \infty$ (see Fig. 1). The result is (13)

$$q_{cl,B} = (2\pi\mu kT/h^2)^{3/2} \times 4\pi \int_{R_-}^{\infty} R^2 dR \, [e^{-U_0(R)/kT} f(A)] \qquad (10)$$

where

$$f(A) = \int_0^A (4y/\pi)^{1/2} e^{-y} dy = \mathrm{erf}(A^{1/2}) - (4A/\pi)^{1/2} e^{-A} \qquad (11)$$

In these equations erf is the error function and $A = [\mathfrak{T}_e - U_0(R)]/kT$. Note that although the exponential term in brackets in Eq. (10) becomes constant as $R \to \infty$, $f(A)$ goes to zero faster than R^{-3} for most potentials (see below), so the integral in Eq. (10) remains bounded.

The classical treatment outlined above requires the potential $U_0(R)$, but nowhere involves the effective potential $U_J(R)$. Thus it is not clear how the metastable contributions to q_{cl} might be calculated, since they are defined specifically in terms of the effective potentials. One could return to an explicit sum over J, with the (one-dimensional) vibrational spectrum treated classically, and presumably regain thereby an explicit evaluation of the metastable contributions. However, this seems pointless, since (a) rotation is generally more classical than vibration, and (b) the calculations are anyway likely to be more time-consuming than the full semiclassical calculations outlined above. Instead, I have examined two other ways of limiting the range of the momentum integration in Eq. (4), to see how closely these account for the metastable contributions. In the first case the three components of momentum are *individually* limited by the maximum allowed kinetic energy. In the second the rotational and vibrational energies are separately limited to $\mathfrak{T}_e - U_0(R)$. For these treatments the quantity $f(A)$ becomes

$$\begin{aligned} &\text{(For 1):} \quad [\mathrm{erf}(A^{1/2})]^3 \\ &\text{(For 2):} \quad (1 - e^{-A})\,\mathrm{erf}(A^{1/2}) \end{aligned} \qquad (12)$$

I will call the corresponding partition functions $q_{cl,1}$ and $q_{cl,2}$. Note that both must be larger than $q_{cl,B}$, since the momentum space is less restricted. For the same reason $q_{cl,1}$ must be greater than $q_{cl,2}$. However, there is still no direct involvement of the effective potential $U_J(R)$, so no obvious relation to the exact $(q_B + q_{AI})$. This connection can only be investigated numerically, and is done so in calculations discussed below.

COMPUTATIONAL METHODS

The semiclassical computations have been described in detail in ref. (5). Briefly they involve evaluating the phase integral of Eq. (2) at specified, equidistant intervals of E between the minimum, E_{min}, and the barrier, E_{max}, for each effective potential $U_J(R)$. The eigenvalues are then estimated by interpolation over the resulting grid of E and (noninteger) v values. A surprisingly small number of E intervals (6–10), together with

low-order Lagarangian interpolation, serve to estimate the important low v levels with spectroscopic accuracy (~0.01 cm^{-1}). (This is because the relationship between E and v is nearly linear at low v). Levels near the top of the well may be considerably more in error (~10 cm^{-1}), but for these levels such errors have little effect on q_{cl}. In any event, their effect can be checked easily by increasing the number of points in the interpolation grid and the order of the interpolation.

To evaluate the classical partition function I have used a Simpson-type integration with higher-order corrections. Since this method involves a grid of equidistant points on the R-axis, it is necessary to specify the upper limit of the integration, R_+. In test calculations I found that the range beyond R = 10 Å made small but systematic contributions, and I elected to estimate these large-R contributions by assuming the potential behaves as $-C_n/R^n$ for $R \geq R_+$, with C_n determined by $\mathfrak{T}_e$ and $U_0(R_+)$. With this assumption the integrand in Eq. (10) takes the limiting form.

$$(4/3\sqrt{\pi})\,(C_n/kT)^{3/2} \exp(-\mathfrak{T}_e/kT)\, R^{(2\,-\,3n/2)} \qquad (13)$$

As long as $n > 2$ (which covers all but ionic interactions: these require special attention in any treatment), the integral of the quantity in Eq. (13) from R_+ to infinity is finite. For the commonly occurring case, $n = 6$, the large-R contribution to the integral in Eq. (10) is

$$(2/9\sqrt{\pi})\,(C_6/kT)^{3/2} \exp(-\mathfrak{T}_e/kT)\, R_+^{-6} \qquad (14)$$

In the corresponding calculations for $q_{cl,1}$ and $q_{cl,2}$ [Eq. (12)], the first factor in Eq. (14) becomes $(4/3)\pi^{-3/2}$ and $(1/3\sqrt{\pi})$, respectively. Since $n = 6$ is appropriate in my test cases, I have used these expressions.

For the Ar_2 calculations I have used the same 6-12 potential employed in Ref. (5).

$$U_0(R) = 7.98 \times 10^5/R^{12} - 5.65 \times 10^5/R^6 \qquad (15)$$

where the units of energy and distance are cm^{-1} and Å, respectively. For this potential $\mathfrak{T}_e$ = 100.01 cm^{-1} and R_e = 3.76 Å, which approximate the current best spectroscopic estimates (14).

For HgBr, recent spectroscopic work on the single isotopic species $^{200}Hg^{79}Br$ has given an improved description of the vibrational structure in the ground state for v = 0–34 (15, 16), and from a partial rotational analysis, the estimate $R_e \approx 2.49$ Å. Without a complete rotation analysis, I am unable to calculate the full RKR curve. Hence I have used a Morse-RKR potential (17), for which the repulsive branch is defined by a Morse curve based on the experimental estimates of R_e and the first two vibrational constants, ω_e and $\omega_e x_e$. The RKR f-integral is then used to evaluate the width of the potential as a function of v, from which the attractive branch is constructed.

The vibrational constants in ref. (16) were obtained from a direct fit to a mixed representation for the ground state—the usual polynominal in

$(v + 1/2)$ for low v levels, a near-dissociation expansion for high v—with smoothness constraints at the switchover point. For the latter we chose $v = 25$, and to insure smoothness we required that both representations agree at $v = 25$ and 26. Although these constraints insure continuity of the function, the first derivative is only *approximately* continuous, as was evident from slow convergence of the RKR calculations for levels just above $v = 25$. Thus I have concluded that it is better to explicitly constrain the function and its first derivative to be continuous at a specified value v. Accordingly I have modified the constants of ref. (*16*) very slightly to achieve this smoothness. The changes are completely insignificant for the present purposes and are mentioned here purely as a technical point. The constants are likely to change somewhat anyway as we extend the assignments to higher v. In this last context it should be noted that although I am using the vibrational constants of ref. (*16*) to define the entire potential curve, the upper region of the curve remains experimentally uncertain, with Σ_e uncertain by ± 75 cm^{-1}. For thermodynamic applications the latter uncertainty remains the limiting factor.

With the above mentioned changes in the smoothness constraints, the RKR calculations were extended to $v = 62$ with no convergence problems. This level is only three quanta below v_D (the vibrational quantum number at dissociation) and 0.5 cm^{-1} below Σ_e (= 5527.2 cm^{-1}), and has a right-hand turning point near 11 Å. The mixed representation for the vibrational energy, $G(v)$, is readily handled by the method I have described previously (*18, 19*), which employs another version of the Gauss-Mehler quadrature (*20*).

In the Simpson's method estimation of the classical phase integral (Eq. 10), the use of a step size $\Delta R = 0.01$ Å agreed with results for $\Delta R = 0.02$ Å to better than one part in 10^4, so no further decrease in step size was needed. For the evaluation of $q_{cl,B}$, $q_{cl,1}$, and $q_{cl,2}$, at ten temperatures, the classical calculations (which could be done in single precision) took about 5 s of CPU time, which was about two orders of magnitude faster than the corresponding semiclassical calculations in the case of HgBr, or one order of magnitude in the case of Ar_2.

RESULTS AND DISCUSSION

The results of the Ar_2 calculations are illustrated in Fig. 2. The semiclassical and classical estimates of the bound contribution to q_{vr} agree too closely to be distinguished in the scale of this plot. (The classical value was 1.1% high at 100 K, decreasing to 0.6% at 800 K.) On the other hand the classical functions, $q_{cl,1}$ and $q_{cl,2}$, sandwich the exact (semiclassical) values for the combined bound and metastable contributions. In fact the average of $q_{cl,1}$ and $q_{cl,2}$ is within 1.5% of the exact value at all T, hence is a reasonably good approximation of the latter.

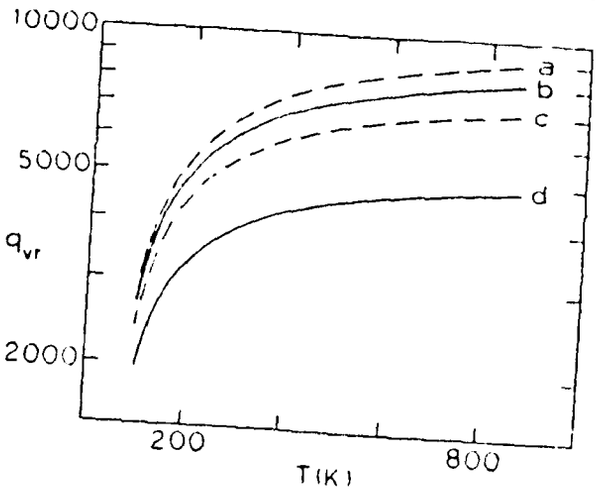

Fig. 2. Comparison of classical and exact partition functions for Ar_2 as a function of T. The plotted quantities are as follows: (a) $q_{cl,1}$, (b) the exact ($q_B + q_M$), (c) $q_{cl,2}$, and (d) $q_{cl,B}$ (≈ the exact q_B).

Unfortunately the last result is not general, as is evident from the HgBr results, shown in Fig. 3. Here $q_{cl,1}$ is reasonably close to ($q_B + q_M$), but it deviates progressively at high T (see curve b). The function $q_{cl,2}$ (not shown) is about halfway between $q_{cl,B}$ and $q_{cl,1}$. Note that again $q_{cl,B}$ (curve b) is within 0.5% of exact except at the low-T end. However, even at 200 K, where kT is only 74% of the vibrational energy, the error is only 4%. From simple considerations of zero-point energies, one might expect the classical result to be in error by as much as a factor of two. The present calculations make it clear that the classical method is in fact much better than has generally been recognized. There is one slightly surprising result in the calculations displayed in Fig. 3: Although the error in the classical approximation to q_B is only 0.35% at 3000 K, it is actually *increasing* with T. I was suspicious of this result, so I checked it by repeating the calculations using a Morse approximation to the HgBr potential. The agreement was better in this case but still not exact, and again the deviation was increasing at high T, but in the opposite direction. This effect may have to do with the manner in which the phase space near the dissociation limit is sampled discretely by the exact partition function.

For completeness I have included in Fig. 3 the comparisons for the exact evaluation of ($q_B + q_M$) for the Morse approximation to the ground state (curve a) and the RR/HO model (curve d). The Morse results are high, because the attractive branch of the potential lies below the "true" (Morse-RKR) curve in its upper region, making more phase space available to bound molecules. The RR/HO partition function drops below the

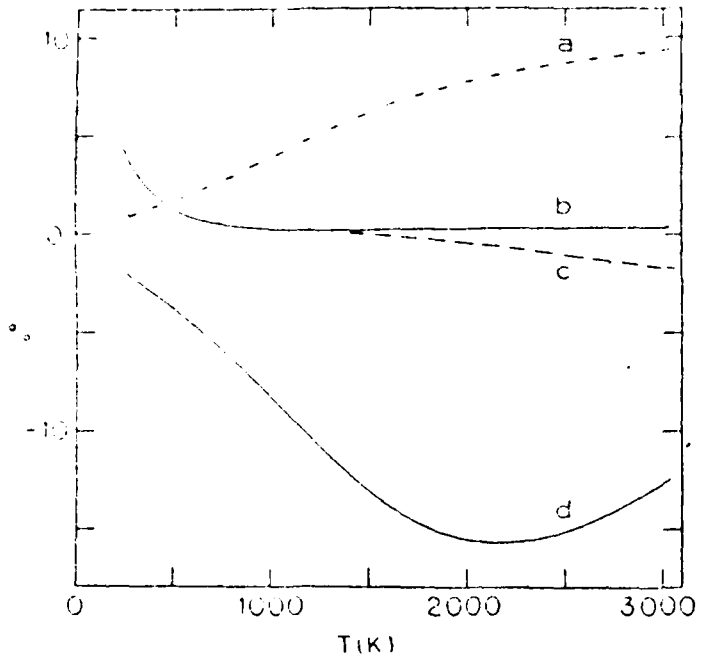

Fig. 3. Percent deviation from exact for various partition functions of HgBr. For curves (a), (c), and (d), the reference is the exact $(q_B + q_{M})$ calculated for the Morse-RKR curve. The quantities compared are: (a) the exact $(q_B + q_{M})$ for the Morse approximation to the ground state potential, (c) the classical function, q_{cl}, and (d) the RRHO partition function. Curve (b) shows the comparison between the classical and exact values of q_B for the Morse-RKR curve.

exact values in this temperature range: however, it is rising at high T, as it must, since the RRHO model assumes an infinite rotational and vibrational spectrum, and consequently the RRHO q_{vr} must exceed the exact q_{vr} at high T (5).

For thermodynamic applications I have experimented with several ways of representing q_{vr} for HgBr and have settled on the expression,

$$\ln (q_{vr}) = 7.485 + 1.615 \ln(y) - 0.877/y + 6.78 \times 10^{-2}y - 1.406 \times 10^{-3}y^2 + 6.96 \times 10^{-6}y^3, \quad (15)$$

where $y = (T/100)$. The constants in this expression were obtained from a least-squares fit of the semiclassical $(q_B + q_{M})$ values for $^{200}Hg^{79}Br$ at T = 200-1200 K in steps of 100 K, extending to 3000 K in steps of 300 K thereafter. The coefficients have been rounded with care, and Eq. (15) reproduces the original q_{vr} values with a maximum deviation of 0.2%. I have verified that this function and its first derivative are "smooth" functions of T over the stated range and somewhat beyond. Note that the reference of energy is the minimum of the potential and that Σ_e is 5527.2 cm^{-1} for this curve. The first constant in Eq. (15) includes ln 2 for the spin degeneracy. For other isotopomers of HgBr this constant can be altered in an obvious way to reflect the $\mu^{-3/2}$ dependence in q_{vr} [Eq. (10)].

CONCLUSION

In this work I have examined the numerical accuracy of the classical method of calculating diatomic rotation–vibration partition functions: As a reference I have used an exact sum over states, with the latter estimated by a semiclassical technique. Test calculations for Ar_2 and HgBr indicate that the classical estimate of the bound partition function, $q_{cl,B}$, is correct within 1% when $kT > 2hc\omega_e$. This performance is much better than is generally recognized. For the estimation of the metastable contribution to q_{vr}, I have tried two other ways of defining the available momentum space in the classical method; but neither has proved fully satisfactory, and it appears that q_M can best be assessed by the semiclassical procedure.

The present calculations have dealt with just the bound and metastable contributions to q_{vr}. However, it seems likely that the classical expression for the full q_{vr}, including the continuum, will be equally reliable and by far the easiest way to evaluate q_{vr} when the molecular continuum is included within the phase space allocated to the molecule (*1, 2*). For the calculation of concentrations of bound and metastable molecules in equilibrium with the parent atoms, however, the partition functions, q_B and q_M, are still of value and can be calculated easily by the methods I have outlined.

For thermodynamic applications I have expressed my results for $^{200}Hg^{79}Br$ in terms of a simple empirical equation, with coefficients determined by the method of least squares. The results in this case are still limited by experimental uncertainties, primarily in the dissociation energy and the sketchy rotational analysis. We are continuing work on the spectroscopy of this molecule and the other HgX diatomics and hope to reduce the remaining uncertainties.

ACKNOWLEDGMENTS

I want to thank Fred Mies and Paul Julienne for several helpful discussions and for sending me a copy of ref. (*1*) prior to its publication. This work was supported by the Office of Naval Research.

REFERENCES

1. Mies, F. H., and Julienne, P. S., *J. Chem. Phys.* **77**, 6162 (1982).
2. Mies, F. H., and Julienne, P. S., to be published.
3. Beckett, C. W., and Haar, L., *Proc. of the Joint Conference on Thermodynamic and Transport Properties of Fluids*, Institute of Mechanical Engineers, London, p. 27 (1957).
4. Haar, L., *Kinetics, Equilibria and Performance of High Temperature Systems*, Proc. of the First Conference of the Western States Section of the Combustion Institute, Butterworth, London, 1959.
5. Tellinghuisen, J., *Chem. Phys. Lett.* **102**, 4 (1983).
6. Tellinghuisen, J., *Chem. Phys. Lett.* **18**, 544 (1973).
7. Hill, T. L., *An Introduction to Statistical Thermodynamics*, Addison-Wesley, Reading, Mass., 1960.
8. Pitzer, K. S., and Brewer, L., *Thermodynamics* (revised from original by G. N. Lewis and M. Randall), McGraw-Hill, New York, 1961.
9. Le Roy, R. J., and Lam, W.-H., *Chem. Phys. Lett.* **71**, 544 (1980).
10. Tromp, J. W., and Le Roy, R. J., *Can. J. Phys.* **60**, 26 (1982).
11. Tellinghuisen, J., *J. Chem. Phys.* **78**, 2374 (1983).
12. Hirschfelder, J. O., Curtiss, C. F., and Bird, R. B., *Molecular Theory of Gases and Liquids*, Wiley, New York, 1954.
13. Hedges, R. E. M., Drummond, D. L., and Gallagher, A., *Phys. Rev. A.* **6**, 1519 (1972).
14. Colbourn, E. A., and Douglas, A. E., *J. Chem. Phys.* **65**, 1741 (1976).
15. Tellinghuisen, J., and Ashmore, J. G., *Appl. Phys. Lett.* **40**, 867 (1982).
16. Tellinghuisen, J., and Ashmore, J. G., *Chem. Phys. Lett.* **102**, 10 (1983).
17. Tellinghuisen, J., and Henderson, S. D., *Chem. Phys. Lett.* **91**, 447 (1982).
18. Tellinghuisen, J., *J. Mol. Spectr.* **44**, 194 (1972).
19. Tellinghuisen, J., *Computer Phys. Commun.* **6**, 221 (1974).
20. Kopal, Z., *Numerical Analysis*, Chapman and Hall, London, 1961.

TABLE I

Assigned Violet-Degraded Bandheads in the $C-X$ System of $^{200}Hg^{127}I$

v'-v''	ν(cm^{-1})	$\Delta\nu$[a]
0- 3	32419.8	0.0
1- 5[b]	420.8	0.3
1- 4	535.0	0.2
0- 2	538.8	-0.1
2- 5	649.5	-0.5
1- 3	651.6	0.1
0- 1	659.9	0.0
3- 6	761.0	-0.5
2- 4	762.9	0.2
1- 2	770.6	0.1
0- 0	783.5	-0.2
4- 7	869.0	-0.2
3- 5	872.4	-0.4
2- 2	998.6	0.0
1- 0	33015.3	0.0
3- 3	102.7	0.0
2- 1	119.9	-0.1
2- 0	243.1	0.1
3- 1	342.5	0.4
4- 2	438.7	0.3
3- 0[b]	466.4	-0.1
4- 1	559.8	0.4
5- 2[b]	650.2	-0.5
5- 1[b]	770.9	0.0

[a] $\nu_{calc} - \nu_{obs}$ from mixed representation fit of all systems.

[b] Assignment weighted 0.33 in least-squares fit.

TABLE II

Assigned Violet-Degraded Bandheads in the $D-X$ System of $^{200}Hg^{127}I$

v'-v''	ν(cm^{-1})	$\Delta\nu$[a]
1-11	35244.7	0.7
1-10	341.7	1.1
2-10	515.4	0.3
1- 8	546.9	-0.3
0- 6	587.6	-0.3
0- 5	698.7	0.1
2- 8	718.8	0.7
1- 6	761.4	0.3
0- 4	812.5	0.4
1- 5	872.8	0.5
0- 3	930.2	-0.7
4- 9	957.5	-0.3
3- 7	996.9	0.1
0- 2	36048.6	-0.1
2- 4	159.9	0.4
0- 1	170.3	-0.6
1- 2	223.0	-0.1
2- 3	277.0	-0.1
5- 7	334.5	0.3
1- 1	344.5	-0.4
4- 5	386.8	0.4
3- 3	448.8	-0.6
1- 0	467.3	0.2
4- 4	501.0	0.3
2- 1	517.4	-0.4
2- 0	640.7	-0.3
5- 4	669.1	0.3
3- 0	812.8	-1.1
4- 0	982.2	-0.8
5- 1	37026.1	0.1

[a] $\nu_{calc} - \nu_{obs}$ from mixed representation fit of all systems.

TABLE V

Franck-Condon Factors ($\times 10^3$) for $C \rightarrow X$ System in $^{200}Hg^{127}I$[a]

v''	$v'=0$	1	2	3	4	5	6	7	8	9	10	11	12
0	364	298	191	91	37	13	4	1	0	0	0	0	0
	330	298	202	103	44	16	5	1	0	0	0	0	0
1	398	0	82	180	161	102	49	19	6	2	0	0	0
	393	4	61	167	167	113	58	24	9	3	1	0	0
2	188	208	87	1	60	135	143	97	50	21	7	2	1
	209	165	105	7	40	121	145	108	60	27	10	3	1
3	45	304	23	94	66	0	52	122	127	90	47	20	7
	59	297	6	84	82	2	33	108	129	101	57	26	10
4	4	152	235	11	21	103	32	1	58	114	117	81	43
	7	179	190	27	9	95	49	0	38	102	121	92	53
5	0	31	253	86	52	5	57	72	20	7	64	113	107
	0	48	259	45	61	16	35	75	36	1	44	102	113
6	1	1	103	253	4	39	55	5	56	64	7	14	75
	1	4	136	217	0	28	69	0	40	72	19	3	54
7	0	2	13	197	150	12	3	82	10	12	70	42	1
	1	1	29	220	96	26	0	72	25	2	57	56	10
8	0	2	0	60	240	40	28	15	47	42	3	33	62
	0	2	0	95	223	11	29	31	24	49	15	14	58
9	0	1	5	3	141	187	0	11	62	5	39	37	1
	0	2	3	14	177	134	5	3	70	0	27	50	2

[a] First entry is for $J'=J''=0$. Second entry is for $J'=J''=100$.

TABLE VI

Franck-Condon Factors ($\times 10^3$) for $D \rightarrow X$ System in $^{200}Hg^{127}I$[a]

v''	$v'=0$	1	2	3	4	5	6	7	8
0	52	164	217	237	163	85	36	12	3
	48	156	242	238	168	91	39	14	4
1	134	192	67	2	86	172	166	106	50
	127	192	74	0	76	166	168	112	55
2	188	81	9	112	80	1	51	140	153
	182	88	5	106	87	3	41	132	155
3	190	4	89	60	6	92	68	1	48
	188	7	81	67	2	85	76	3	38
4	157	16	94	0	81	36	13	89	51
	158	12	96	0	75	43	7	83	60
5	112	65	35	45	51	10	77	13	29
	115	57	41	37	58	5	75	21	19
6	72	99	1	77	1	65	16	32	63
	76	93	2	74	3	59	24	23	67
7	43	104	14	50	23	45	12	60	0
	46	102	9	55	16	51	6	61	3
8	24	89	46	12	58	3	54	8	40
	27	90	39	17	53	7	48	15	31
9	13	67	70	0	53	11	41	11	46
	15	70	64	0	56	6	46	5	50
10	7	46	77	16	24	41	6	45	5
	8	49	74	10	30	34	12	38	12
11	4	29	70	38	3	49	4	39	9
	4	32	70	31	6	48	1	43	3

[a] First entry is for $J'=J''=0$. Second entry is for $J'=J''=100$.

TABLE VIII

Assigned Red-Degraded Bandheads in the $G-X$ System of $^{200}Hg^{[57]}$

v'-v''	ν(cm^{-1})	$\Delta\nu$[a]
6-12	44733.3	-0.7
5-11	740.1	-0.5
4-10	750.6	-0.4
3- 9	763.5	-0.1
2- 8	779.4	0.0
1- 7	797.6	0.4
7-12	819.5	-0.1
5-10	836.9	0.4
4- 9	850.6	0.0
3- 8	867.0	-0.2
2- 7	885.8	-0.2
1- 6	906.6	0.4
2- 6	994.8	-0.3
1- 5	45018.1	0.4
0- 4	045.3	-0.3
4- 7	060.4	-0.2
2- 5	106.4	-0.3
1- 4	132.4	0.3
0- 3	161.8	-0.2
3- 5	193.8	-0.4
0- 2	280.7	-0.2
3- 4	307.3	0.3
2- 3	336.2	0.6
1- 2	367.6	0.6
0- 1	402.2	-0.5
1- 1	489.7	-0.3
3- 2	542.7	0.4
2- 1	576.8	0.1
5- 3	597.9	0.6
1- 0	612.5	0.3
4- 2	630.3	0.0
7- 4	655.7	-0.1
2- 0	700.3	0.0
8- 4	712.3	0.0
4- 1	751.6	-0.1
3- 0	45787.7	0.0
5- 1	838.4	0.2
8- 3	858.5	0.4
4- 0	874.9	0.0
6- 1	925.4	0.2
5- 0	962.2	-0.2
8- 2	977.5	0.3
7- 1	46011.8	0.6
6- 0	049.3	-0.4
8- 1	099.4	-0.4
7- 0	135.7	0.1

[a] $\nu_{calc} - \nu_{obs}$ from mixed representation fit of all systems.

TABLE IX

Assigned Red-Degraded Bandheads in the $F_3 \rightarrow X$ System of $^{200}Hg^{127}I$

v'-v''	ν(cm^{-1})	Δ_c[a]
6-18	42846.2	-1.2
6-17	917.8	0.8
1-12	941.4	-0.3
7-17	993.4	-0.7
6-16	996.0	-0.1
5-15	43000.7	0.1
3-13	014.6	0.7
2-12	024.4	0.2
1-11	034.7	0.7
0-10	047.6	-0.3
10-19	059.8	0.4
8-17	065.5	-0.5
6-15	076.7	0.1
3-12	106.5	-0.2
2-11	118.0	0.9
11-19	126.7	0.1
9-17	135.5	-0.2
8-16	141.5	0.8
0-9	147.9	-0.2
6-14	161.3	-0.1
5-13	173.8	-0.8
3-11	199.9	0.7
2-10	216.3	0.0
1-9	233.0	0.2
6-13	249.8	-0.8
0-8	250.0	1.1
5-12	264.9	-0.8
8-14	307.1	0.5
2-9	317.3	-0.5
1-8	336.3	0.2
0-7	358.4	-1.2
1-7	442.7	0.0
5-10	456.3	-0.6
0-6	466.6	-0.4
1-6	551.4	0.2
5-9	43555.9	0.3
0-5	577.3	0.4
2-6	635.0	0.2
1-5	661.6	-1.4
0-4	691.2	0.6
3-6	716.3	0.6
2-5	746.2	0.6
0-3	808.9	-0.5
3-5	827.8	0.7
1-3	894.2	-0.3
3-4	942.0	0.6
1-2	44013.1	-0.3

[a] $\nu_{calc} - \nu_{obs}$ from mixed representation fit of all systems.

TABLE VII

Assigned Red-Degraded Bandheads in the $H \rightarrow X$ System of $^{200}Hg^{127}I$

v'-v''	ν(cm^{-1})	$\Delta\nu$[a]
2-11	46061.9	0.9
2-10	160.0	0.2
2- 9	260.5	0.1
1- 8[b]	274.4	0.3
2- 8	364.1	-0.1
1- 7	380.7	0.1
0- 6	394.8	0.1
1- 6	490.0	-0.2
0- 5	506.8	-0.4
1- 5	601.3	0.0
0- 4	620.5	0.0
2- 5	691.3	-0.7
1- 4	715.7	-0.3
0- 3	737.1	0.0
2- 4	805.0	-0.3
1- 3[b]	831.5	0.5
0- 2	855.9	0.2

[a] $\nu_{calc} - \nu_{obs}$ from mixed representation fit of all systems.

[b] Assignment weighted 0.25 in least squares fit.

TABLE XX

Spectroscopic Parameters (cm^{-1}) for $^{200}Hg^{127}I$[a]

	$X(^2\Sigma^+)$	$B(^2\Sigma^+)$	$C(^2\Pi_{\frac{1}{2}})$	$D(^2\Pi_{\frac{3}{2}})$
T_e	0.0	24072.44 (18)	32728.53 (27)	36267.73 (27)
T		21275.28 (9.0)		
D_e	2797.2 (9.0)			
c_{v1}	125.48 (4)	110.92 (7)	235.25 (42)	176.04 (21)
c_{v2}	-1.0186 (59)	-0.172 (6)	-1.4 (2)	-0.79 (3)
c_{v3}	$-1.56\ (2) \times 10^{-2}$		-0.14 (2)	
v_d	60.4 (3)			
X_6	0.0108			
a_3	$1.60\ (19) \times 10^{-6}$			
σ	0.38			

[a]Results from fit to mixed representation for X state- polynomial for $v \leq 20$, NDE for $v \geq 20$. The correction function of the NDE is of the form $F = 1.0 + a_3(v_d - v)^3$.

TABLE XX

Spectroscopic Parameters (cm^{-1}) for $^{200}Hg^{127}I$[a]

	F_3	G	H
T_e	44191.01 (19)	45543.71 (16)	47113.61 (29)
T			
D_e			
c_{v1}	87.37 (8)	87.81 (7)	100.5 (5)
c_{v2}	-0.946 (8)	-0.072 (7)	-2.8 (1)

TABLE I

Estimated Band Origins (cm^{-1}) of Assigned Bands of $B-X$ System of $^{200}HgBr$

$v'-v''$[a]	$\nu(Hg^{79}Br)$	$\Delta\nu$[b]	Weight[c]	$\nu(Hg^{81}Br)$[d]	$\Delta\nu$[b]
6-34	19508.2	0.7	1.0		
7-35	575.0	-0.4	1.0		
2-27	602.5	0.2	1.0		
5-31	613.2	0.1	1.0		
(3-28)	633.3				
6-32	661.8	0.1	1.0		
1-25	691.2	0.3	1.0		
8-35	707.4	-0.9	1.0		
2-26	712.2	0.3	1.0		
7-33	714.8	-0.5	1.0		
3-27	737.0	0.2	1.0		
4-28	765.7	0.1	1.0		
5-29	799.3	-0.5	1.0		
1-24	809.5	0.1	1.0		
2-25	826.2	0.3	1.0		
6-30	837.3	-0.8	1.0		
3-26	846.8	0.1	1.0		
4-27	871.6	-0.5	1.0		
7-31	878.9	-0.3	1.0		
9-34	901.5	0.6	1.0		
0-22	922.4	0.0	1.0		
1-23	932.0	-0.2	1.0		
2-24	941.3	0.3	1.0		
7-30	968.9	0.0	1.0		
8-31	20011.1	-0.5	1.0		
0-21	052.1	0.1	10.0		
1-22	057.6	0.3	1.0		
10-33	108.7	0.6	1.0		
0-20	185.8	0.0	10.0	20209.8	0.0
3-23	201.3	0.0	1.0		
0-19	322.9	-0.2	10.0	346.2	0.1
5-24	346.7	-0.3	1.0		
0-18	463.0	0.0	10.0	485.7	0.2
3-20	590.6	0.0	1.0		
1-18	598.9	-0.4	1.0	620.3	-0.1
0-17	606.8	-0.1	1.0	629.1	-0.4
3-19	727.2	0.4	1.0		
1-17	743.1	-0.9	1.0	763.0	0.0
2-17	20877.6	-0.5	1.0		
1-16	888.7	0.3	1.0	20909.5	-0.5
4-18	21002.5	-0.6	1.0		
2-16	024.1	-0.2	1.0	21042.9	-0.2
1-15	038.8	0.0	1.0		
7-20	123.2	0.1	1.0		
2-15	174.2	-0.5	1.0		
1-14	21191.8	-0.2	1.0		
5-17	278.6	0.4	1.0		
3-15	308.4	-0.2	1.0		
2-14	326.1	0.4	1.0	21343.6	-0.1
1-13	346.7	0.5	1.0		
5-16			1.0	440.7	0.3
4-15	441.8	0.3	1.0		
3-14	461.1	-0.1	1.0	477.1	-0.4
2-13	482.2	0.0	1.0		
8-18	531.8	0.7	1.0		
6-16	558.2	0.4	1.0		
4-14	594.7	0.2	1.0		
3-13	616.5	0.1	1.0	631.3	0.0
2-12	639.9	0.7	1.0		
4-13	750.7	-0.1	1.0		
3-12	774.9	0.1	1.0		
9-17	807.1	0.4	1.0		
7-15	840.6	0.3	1.0		
5-13	883.9	0.1	1.0		
4-12	908.8	0.2	1.0	921.5	-0.1
3-11	936.3	-0.2	1.0		
(6-13)	22018.2				
5-12	042.4	0.0	1.0	22053.4	0.3
4-11	070.0	0.1	1.0		
6-12	175.6	-0.3	1.0	185.5	-0.1
5-11	203.5	0.0	1.0	213.6	0.0
6-11	336.2	0.2	1.0	345.3	0.1
7-11	468.7	0.1	1.0		
6-10	499.9	0.2	1.0		
8-11	600.3	0.4	1.0		
7-10	632.4	0.1	1.0		

v'-v''[a]	ν($Hg^{79}Br$)	$\Delta\nu$[b]	Weight[c]	ν($Hg^{81}Br$)[d]	$\Delta\nu$[b]
6-9	22566.7	-0.3	1.0		
8-10	764.5	-0.1	1.0		
7-9	798.9	-0.2	1.0		
9-9	23061.6	0.4	1.0		
8-8	098.7	0.7	1.0		
10-9	193.4	-0.6	1.0		
9-8	230.4	0.3	1.0		
(11-9)	324.2				
10-8	362.6	-1.1	1.0		
9-7	402.9	-1.1	1.0		
11-8	492.5	-0.7	1.0		
10-7	533.0	-0.3	1.0		
12-8	621.2	0.4	1.0		
11-7	663.3	-0.3	1.0		
13-8	749.9	1.0	1.0		
13-7	922.5	-0.5	1.0		
13-6	24095.4	0.2	1.0		

[a]Assignments in parentheses were not included in the least-squares fit.

[b] $\nu_{calc} - \nu_{obs}$ from final, simultaneous least-squares fit of all systems.

[c]All bands of $^{200}Hg^{81}Br$ are weighted the same as those in $^{200}Hg^{79}Br$ except 0-18 which has a weight of 1.0.

[d]Measured using a source made from natural Br_2.

TABLE III

Assigned Bandheads in the $C \rightarrow X$ System of $^{200}Hg^{81}Br$

v'-v''	ν(cm^{-1})	Weight[a]	$\Delta\nu$[b]
0-3	31218.4	0.33	-0.1
1-4	309.0	0.33	0.3
0-2	399.3	0.33	-0.1
1-3	487.8	0.33	0.3
0-1	582.4	0.33	-0.2
1-2	668.7	0.33	0.3
0-0	767.5	0.33	-0.1
5-7	855.7	0.33	-0.5
1-0	35036.8	0.33	0.4
4-4	117.4	0.33	0.0
5-5	200.8	0.33	0.9
3-1	391.7	0.33	-1.3
5-3	556.5	0.33	0.6
6-4	631.2	0.33	-0.3
5-2	737.8	0.33	0.2
6-3	809.8	0.33	-0.2

[a]Weight used in the final, simultaneous least-squares fit of all systems.

[b] $\nu_{calc} - \nu_{obs}$ from final, simultaneous least-squares fit of all systems.

TABLE II

Assigned Bandheads in the $D \rightarrow X$ System of $^{200}Hg^{81}Br$

v'-v''	ν(cm^{-1})	Weight	$\Delta\nu$[a]
5-15	37172.0	1.0	-0.8
6-16	240.5	1.0	-0.7
4-13	259.1	1.0	-1.0
2-10	293.0	1.0	0.2
5-14	323.0	1.0	0.0
3-11	353.9	1.0	0.1
6-15	388.7	1.0	0.0
1-8	400.2	1.0	0.1
4-12	415.7	1.0	-0.2
2-9	457.4	1.0	0.8
5-13	478.0	1.0	-0.4
3-10	516.8	1.0	-0.3
6-14	540.7	1.0	-0.2
1-7	570.2	1.0	-0.1
4-11	575.1	1.0	0.3
2-8	625.3	1.0	0.3
4-10	737.7	1.0	0.2
1-6	741.7	1.0	0.5
2-7	795.2	1.0	0.2
3-8	848.7	1.0	0.2
0-4	866.3	1.0	-0.4
1-5	916.3	1.0	0.3
2-6	967.1	1.0	0.4
3-7	38918.8	1.0	-0.1
0-3	045.4	1.0	-0.7
1-4	093.4	1.0	-0.3
2-5	141.9	1.0	-0.1
6-10	173.9	1.0	1.0
0-2	225.7	1.0	-0.1
1-3	272.7	1.0	-0.7
6-9	340.1	1.0	-0.2
3-5	365.1	1.0	0.1
0-1	408.4	1.0	0.3
5-7	458.8	1.0	0.8
2-3	497.1	1.0	0.1
3-4	511.8	1.0	0.0
4-5	585.5	1.0	0.1

v'-v''	ν(cm^{-1})	Weight	$\Delta\nu$[a]
0-0	38594.1	1.0	-0.3
1-1	636.1	1.0	-0.2
2-2	678.1	1.0	0.0
7-8	722.3	1.0	0.6
8-9	769.0	1.0	0.1
1-0	820.6	1.0	0.4
6-6	849.2	1.0	0.0
7-7	892.6	1.0	0.0
3-2	901.8	1.0	-0.3
4-3	941.9	1.0	0.1
5-4	982.9	1.0	-0.3
2-0	39046.1	1.0	0.2
3-1	084.6	1.0	-0.1
6-4	200.0	1.0	0.1
7-5	239.6	1.0	-0.5
3-0	269.1	1.0	0.6
4-1	305.9	1.0	0.0
5-2	342.3	1.0	0.0
4-0	400.4	1.0	0.7
5-1	525.6	1.0	-0.2
6-2	559.8	1.0	0.0
7-3	594.3	1.0	0.2
8-4	630.0	1.0	-0.7
6-1	743.1	1.0	-0.2
7-2	775.8	1.0	-0.4
8-3	808.0	1.0	0.1
9-4	841.0	1.0	0.0
10-5	874.4	1.0	-0.3
11-6	907.6	1.0	-0.1
8-2	988.9	1.0	0.1
9-3	40019.3	1.0	0.5
11-5	081.9	1.0	0.0
12-6	113.3	1.0	0.1
13-7	145.0	1.0	0.2
14-8	177.3	1.0	0.0

[a] $\Delta\nu = \nu_{obs} - \nu_{calc}$ from final, simultaneous least-squares fit of all systems.

TABLE IV

Spectroscopic Parameters (cm^{-1}) for $^{200}Hg^{79}Br$[a]

	$X(^2\Sigma^+)$	$B(^2\Sigma^+)$	$D(^2\Pi_{\frac{3}{2}})$	$C(^2\Pi_{\frac{1}{2}})$
T_e	0.0	23488.93 (24)	38572.81 (20)	34727.14 (69)
T		18005.60 (12.09)		
D_e	5483.3 (12.1)			
c_{v1}	188.913 (92)	136.008 (41)	231.236 (48)	268.42 (97)
c_{v2}	-1.058 (15)	-0.258 (3)	-0.990 (4)	2.6 (3)
c_{v3}	$-1.98\ (88)\times10^{-3}$			-0.42 (3)
c_{v4}	$-2.3\ (2)\times10^{-4}$			
v_d	63.94 (35)			
X_6	0.0186343			
a_1	$2.280\ (271)\times10^{-5}$			
a_2	$-4.34\ (59)\times10^{-7}$			
σ		0.36		

[a]Results from fit to mixed representation for X state- polynomial for $v \leq 26$, NDE for $v > 26$. The correction function of the NDE is of the form $F = 1.0 + a_1(v_d - v)^3 + a_2(v_d - v)^4$.

TABLE VII

Rotational Parameters (cm^{-1}) for the HgBr $B \rightarrow X$ System.[a]

	$^{200}Hg^{79}Br$	$^{200}Hg^{81}Br$
ν_{0-18}	20463.04 (1)	
ν_{0-19}	203222.92 (2)	20346.16 (2)
ν_{0-20}	20185.75 (1)	20209.83 (1)
ν_{0-21}	20052.14 (2)	
$B_{v'}$	0.031838 (19)	0.031132 (24)
$B_{v''}$ (18)	0.041747 (19)	
$B_{v''}$ (19)	0.041413 (20)	0.040585 (24)
$B_{v''}$ (20)	0.040996 (19)	0.040214 (24)
$B_{v''}$ (21)	0.040547 (26)	
$D_{v'}$	7.02×10^{-9}	6.77×10^{-9}
$D_{v''}$ (18)	$1.61\ (4)\times10^{-8}$	
$D_{v''}$ (19)	$1.98\ (4)\times10^{-8}$	$1.89\ (4)\times10^{-8}$
$D_{v''}$ (20)	2.10×10^{-8}	2.0×10^{-8}
$D_{v''}$ (21)	$2.30\ (31)\times10^{-8}$	
σ	0.062	0.070

[a]Distortion Constants for the upper state and for $v'' = 20$ were held constant in the least-squares fit.

END

FILMED

4-85

DTIC